

**Implementation of a Simple Biaxial Concrete Model for
Reinforced Concrete Membranes**

by

Bernardo Garcia Ramirez

A thesis submitted in partial fulfillment of the requirements for the degree of

Master of Science

in

STRUCTURAL ENGINEERING

Department of Civil and Environmental Engineering

University of Alberta

© Bernardo Garcia Ramirez, 2017

ABSTRACT

Although significant progress in the modelling of the nonlinear response of reinforced - concrete (RC) structures at the element level has been achieved in the past decades, reliable and accurate analysis models at the system level for RC structures are scarce. Due to the complexity of elements required to model the 3D response of RC panels, nonlinear analysis of complete RC structures is avoided and instead the response of selected sub-assemblies, isolated from the rest of the structure, is examined in usual design practice. As a result, there is substantial uncertainty on the response of complete RC buildings, making it impossible to analyse global failure modes and making the design more complicated and potentially unsafe. Although simple structures can be designed and analysed based on the response of their components with good accuracy, RC shear wall buildings with complex geometries or under extreme loading necessitate the analysis of the full structure. Recent progress in the development of efficient element formulations to simulate the nonlinear in-plane and out-of-plane response of RC panels, and the availability of experimental data on the response of full shear wall structures, offers the possibility of developing reliable and efficient analysis models for entire RC structures under static and dynamic loads.

This research discusses the advantages and disadvantages of some of the most prominent biaxial element formulations for the nonlinear finite element analysis (FEA) of RC structures. After the assessment, the Mazars concrete material, a damage-based model, is adapted for the use in finite element analysis in plane-stress multilayer-shell elements. The element formulations are implemented in the OpenSees framework, an object-oriented and

open-source framework for simulating applications in earthquake engineering using finite element methods. Finally, the new Mazars model is used to perform quasi-static, reversed cyclic and dynamic analysis of specimens found in literature, and the analytical results are verified with the test data.

ACKNOWLEDGEMENTS

I would like to express my sincere gratitude to Dr. Carlos Cruz Noguez for his invaluable help, technical guidance, and encouragement during the course of this research. Special thanks are due to Dr. Carlos Cruz Noguez, Dr. Samer Adeeb, and Dr. Douglas Tomlinson for serving on the examination committee.

This research was funded by Mexico's National Commission of Science and Technology (CONACYT) and the University of Alberta. I would also like to acknowledge the valuable and kind assistance received to conduct this project from the Norman & Tess Reid Family.

Finally, I am eternally indebted to my family and friends for their love, encouragement, and assistance, without which this research would not have been possible.

TABLE OF CONTENTS

ABSTRACT.....	ii
ACKNOWLEDGEMENTS	iv
LIST OF TABLES	viii
LIST OF FIGURES	ix
CHAPTER 1 – INTRODUCTION	1
1.1 Problem Definition.....	1
1.2 Objective and Scope.....	5
CHAPTER 2 – BACKGROUND AND LITERATURE REVIEW	8
2.1 Introduction.....	8
2.2 Uniaxial Behaviour of Concrete.....	9
2.3 Uniaxial Concrete Models.....	12
2.3.1 Hognestad Model.....	13
2.3.2 Kent and Park Model.....	14
2.3.3 Tensile Model for Concrete	15
2.4 Biaxial Behaviour of Concrete.....	16
2.5 Biaxial Concrete Models.....	18
2.5.1 Total-Strain Models.....	18
2.5.2 Damage-Based Models.....	25

2.6 Structural Simulation Using the Finite Element (FE) Method.....	26
2.6.1 Abaqus FEA	27
2.6.2 VecTor2	29
2.6.3 OpenSees	30
CHAPTER 3 – DAMAGE MODEL FOR CONCRETE.....	32
3.1 Introduction	32
3.2 Mazars Model.....	34
3.2.1 Analysis Procedure	35
3.3 Predictions and Comparison with FEA.....	44
3.3.1 Software Used for Comparison	45
3.3.2 Model Description and Results.....	46
3.4 Development of a Nonlinear 2D Material Model in the OpenSees Interface	49
3.4.1 OpenSees	50
3.4.2 Coordinate System.....	51
3.4.3 Material Constitutive Matrix	52
3.4.4 Analysis Procedure of Concrete Plane Stress Structures.....	54
3.5 New ND Material Model in the OpenSees Framework	57
3.5.1 Methodology. Adding a New Multi-Dimensional Material, nDMaterial.....	57
3.6 Summary	63
CHAPTER 4 – VERIFICATION.....	64

4.1 Introduction	64
4.2 Analysis of a RC Beam Under Monotonical Loading	64
4.2.1 FEA Model and Analysis Method	66
4.2.2 Comparison of Predictions and Experimental Results	67
4.3 Analysis of a RC Shear Wall Under Cyclic Loading.....	68
4.3.1 FEA Model and Analysis Method	69
4.3.2 Comparison of Predictions and Experimental Results	72
4.4 Analysis of a Full-Scale Four-Story RC Building Under Seismic Loading	73
4.4.1 FEA Model and Analysis Method	78
4.4.2 Comparison of Predictions and Experimental Results	80
4.5 Summary	84
Chapter 5 – SUMMARY, CONCLUSIONS AND FUTURE WORK	86
5.1 Summary	86
5.2 Conclusions	87
5.3 Future Work	89
REFERENCES.....	90
APPENDIX A – ‘MAZARS’ SOURCE CODE.....	97

LIST OF TABLES

Table 4.1. List of reinforcing steel (Nagae et al. 2011b)	76
Table 4.2. RC building actual material properties (Nagae et al. 2011b)	77
Table 4.3. Maximum roof drifts for RC building	84

LIST OF FIGURES

Figure 2.1. Typical plot of stress vs. axial strain	10
Figure 2.2. Uniaxial compressive response with unloading and reloading paths at different strains (Hsu and Mo, 2010)	11
Figure 2.3. Compressive stress-strain curve for different concrete strengths (Attard et al., 1986)	12
Figure 2.4. Compressive stress-strain curve (Hognestad, 1951)	13
Figure 2.5. Compressive stress-strain curve from Kent and Park (1971)	15
Figure 2.6. Tensile stress-strain relationship of concrete	16
Figure 2.7. Biaxial behaviour of concrete (Ebead and Neale, 2005)	17
Figure 2.8. Decomposition of a RC element	19
Figure 2.9. Change in subsequent crack angles	19
Figure 2.10. Summary of MCFT for reinforced concrete (Vecchio and Collins, 1986) .	22
Figure 2.11. Summary of CSMM for reinforced concrete (adapted from Mansour and Hsu, 2005)	25
Figure 3.1. Elastic material vs. Damage material	33
Figure 3.2. Use of tensile principal strains to describe any state of strains	36
Figure 3.3. Influence of parameter A_t	39
Figure 3.4. Influence of parameter B_t	40
Figure 3.5. Influence of parameter A_c	41
Figure 3.6. Influence of parameter B_c	41
Figure 3.7. Uniaxial stress-strain response of Mazars model	43

Figure 3.8. Stress-strain response of 1 plain concrete element subjected to pure compression.....	46
Figure 3.9. Stress-strain response of 1 plain concrete element subjected to pure tension	47
Figure 3.10. Force-displacement of 1 plain concrete element subjected to a lateral load	48
Figure 3.11. Force-displacement of 4 plain concrete elements subjected to a lateral load	49
Figure 3.12. Multi-layered shell element.....	51
Figure 3.13. Coordinate systems for concrete elements.....	51
Figure 3.14. Nonlinear analysis algorithm.....	56
Figure 3.15. OpenSees Class Hierarchy. a) OpenSees application Solution, and b) Classes hierarchy.....	58
Figure 4.1. Beam geometric details. Dimensions in mm.....	65
Figure 4.2. FEA model of RC beam	66
Figure 4.3. Analysis results of RC beam	67
Figure 4.4. Shear wall geometric details (Hiotakis, 2004)	69
Figure 4.5. FEA model of RC shear wall.....	71
Figure 4.6. Cyclic analysis results of RC shear wall	73
Figure 4.7. RC building geometric details (Nagae et al. 2011b)	74
Figure 4.8. Input ground motions	78
Figure 4.9. FEA model of RC building.....	79
Figure 4.10. Transverse (T) and Longitudinal (L) directions of RC building	81
Figure 4.11. RC building base shear measured and calculated with 25% Kobe in a) longitudinal, and b) transverse directions	82

Figure 4.12. RC building base shear measured and calculated with 50% Kobe in a)
longitudinal, and b) transverse directions 83

Figure 4.13. RC building base shear measured and calculated with 100% Kobe in a)
longitudinal, and b) transverse directions 83

CHAPTER 1 – INTRODUCTION

1.1 Problem Definition

The economy, availability, high compressive strength, durability, fire-resistance, and stiffness of concrete materials, coupled with the use of steel reinforcement to overcome its low tensile strength, have allowed for the height, overall size and complexity of reinforced - concrete (RC) structures to increase significantly in the last century. This, in turn, makes the forces affecting the structure more difficult to determine.

Accurate and reliable structural analysis is essential to ensure safety and economy, especially with structures with complex geometries or under extreme loading such as seismic events. Usual design practice consists of using linear-elastic analysis software to examine the response of the structure under different loading scenarios. For high-importance buildings or unusual/extreme loads, a more refined tool consists of using nonlinear analysis, in which the nonlinear behaviour of steel and concrete materials is taken into account. Nonlinear analysis, evidently, is more accurate than linear-elastic analysis, but its high cost is prohibitive – in consequence, nonlinear analysis is usually reserved only to study the behaviour of selected sub-assemblies, and suitable boundary conditions are used to simulate the rest of the structure. Such an analysis, of course, would not yield the same level of accuracy of a nonlinear 3D analysis conducted at the system level.

Although simple structures can be designed and analysed based on their linear-elastic response with good accuracy, some effects that may be overlooked include bi-directional moments, torsional effects, and second order effects. Important response parameters in

seismic design, such as ductility reserve, rotational capacity at plastic hinges, and energy dissipation, cannot be calculated. The effects of reversed, cyclic loading must also be considered, as the elements may experience rapid periods of tension and compression stresses. Concrete and steel may exhibit strain-rate effects that cannot be captured with simple linear analysis.

To conduct a nonlinear finite-element analysis at the system level, the finite-element method (FEM) has arisen as a convenient, reliable and versatile computational tool. The constitutive, equilibrium and compatibility equations that arise from the nonlinear stress - strain behaviour of concrete and steel can be solved using iterative solution algorithms until convergence is achieved with acceptable accuracy. The material constitutive relationships developed for the use in FEA, the vast availability of element formulations and solution schemes, and increasing computational power, make it possible to perform finite element analysis of complex reinforced concrete structures with good accuracy. However, although a number of research-oriented and commercially-available finite-element programs are available to conduct this type of studies, programs able to conduct the nonlinear analysis of a full structure are few – most are suited to the study of subassemblies rather than whole structures, while others implement advanced concrete models that inevitably lead to accumulation of numerical errors when the number of elements is large.

The finite element analysis of a 3D RC structure necessitates the use of formulations for the behaviour of concrete in three dimensions, but such formulations are complex given the orthotropic and nonlinear nature of concrete. Certain simplifications in FE models can be made where one or two of the dimensions of a structural member are significantly larger

than the rest. Elements where the longitudinal dimension is significantly larger than the two transverse dimensions (e.g. beams and columns), can be modelled using 1-dimensional (fiber) elements. Similarly, elements with two dimensions significantly larger than the third one (e.g. plates, walls and slabs), can be modelled employing 2-dimensional (shell) elements with a defined thickness. The stress and strain corresponding to the out-of-plane axis are recovered through piecewise integration through the thickness of the shell element.

Considerable research has gone into developing element formulations that can resemble the behaviour of concrete for the use in fiber and shell elements. Analytical models for the uniaxial behaviour of concrete have been successfully implemented into the FE framework for the use in fiber elements, and have been shown to provide accurate results when modelling elements such as beams and columns.

Modelling the biaxial behaviour of concrete is more complex, and has become a very active research topic in the last two decades. Total-strain based models, such as the Modified Compression Field Theory (MCFT) (Vecchio and Collins, 1986), and the Cyclic Softened Membrane Model (CSMM) (Mansour and Hsu, 2005), were developed to describe the behaviour of reinforced concrete biaxial elements. These formulations give accurate results but their solutions require an iterative procedure within the elemental analysis, which increases the possibility of convergence problems when a full structure is analysed.

Other researchers have described the biaxial behaviour of concrete using simpler, damage - based material models such as the Mazars model (Mazars, 1986), where the constitutive law of concrete is expressed as an elastic relationship but modifying the initial stiffness with a scalar damage parameter D that ranges from 0 for the undamaged material to 1 which represents failure of the material. Damage-based material models have shown

to accurately represent the behaviour of concrete in two and three dimensions, while keeping simplicity in their formulations. The material formulations are expressed as explicit equations. Thus, they do not require an iterative procedure to solve them, making the implementation and use of these formulations in FEA a simpler and a more computationally efficient procedure.

Element formulations for the biaxial behaviour of concrete have been implemented in the finite element method. The MCFT was implemented in the program VecTor2, showing a very accurate description of the behaviour of structures that can be modelled using 2D, four-node quadrilateral elements. Abaqus FEA (2009) implements a concrete damaged plasticity model with the assumption of an isotropic damage for the use in 3D RC elements. A damage-based concrete material model has been implemented (Lu et al. 2015) in the OpenSees framework (Fenves, 2001), which can be used in multilayer-shell elements.

But these programs have certain disadvantages. VecTor2 cannot perform analysis in a 3D environment, nor can it be used to model a full structure due to the relatively small number of elements allowed by the program. This makes it not suitable for the analysis at the system level of a RC structure. In what pertains to the programs that allow the nonlinear simulation of full structures, Abaqus FEA has versatile static and dynamic methods for full structures, its source code does not allow the modification or addition of new analysis modules, which makes difficult for researchers to implement the latest results or to verify the theory behind the code. This makes it impossible to analyse engineering phenomena not considered before, or to analyze the behavior of a newly-found material. On the other hand, the open source finite-element platform OpenSees allows for the development of any number of element, material and analysis formulations, and was written specifically to

handle seismic analyses – however, research groups that develop biaxial concrete materials for this framework usually make their source code proprietary and thus key aspects of their performance are unknown.

Based on the preceding discussion, there is a need to develop a simple, robust, yet reasonably accurate biaxial model for concrete in a finite-element platform that allows for the seismic analysis of full RC structures. The material model needs to be simple to allow for a computationally efficient analysis, with minimal convergence problems, and have sufficient accuracy to ensure safe and economic designs. Similarly, the platform in which the material formulations are to be implemented needs to be accessible for researchers to easily adopt new or refined analysis techniques.

1.2 Objective and Scope

The overall objective of this research is to implement a nonlinear material model for the behaviour of concrete in two dimensions, that is simple enough for modelling RC structures at the system level, yet reasonably accurate. The implementation of the material formulations needs to be done in a FEA framework that allows the users to not only use, but to expand and modify this material model with new analysis techniques and innovative materials.

The material model should be able to describe the behaviour of concrete in two dimensions and used in both static and dynamic analyses. The ability to represent the residual strain of the concrete when subjected to cyclic loading, and an explicit relationship for shear are not part of this study, however, but can be addressed in future work.

Within this objective, specific objectives will be pursued in this research:

- An element formulation will be selected after the assessment of some of the most prominent theories that attempt to describe the behaviour of concrete and reinforced concrete in two dimensions. Chapter 2 presents a literature review and the background of finite element modeling and analysis of reinforced concrete structures. The chapter begins by presenting an overview of the properties of concrete, its challenges and unique characteristics under uniaxial loading and biaxial loading. The advantages and disadvantages of some of the most prominent analytical models for concrete in 2D, as well as their applicability, are discussed. The chapter ends by presenting a few FEA programs and frameworks that accurately describe the behaviour of RC structures, with an emphasis in the object - oriented finite element framework, OpenSees.
- The Mazars concrete damage material will be adapted for the use in finite element analysis, in plane-stress multilayer-shell elements. Then, the Mazars model will be implemented in the OpenSees framework for the use in analysis of RC structures. Chapter 3 explains in detail the proposed nonlinear finite element analysis material model for concrete plane structures. The chapter gives the generalities, definitions and the theoretical framework for the Mazars concrete damage material model. The influence of the variables of the model on the concrete response are discussed. Finally, the chapter explains the adaptation of the model in C++ language for the implementation in the OpenSees framework.
- The new Mazars material model will be used in biaxial elements to model different types of structures under various loading conditions, and compared with test results

from the literature to verify its validity. Chapter 4 presents the validation by experimental data of the Mazars concrete damage material model implemented in OpenSees. Three examples, including a beam tested at the University of Alberta under monotonic shear, a shear wall under axial compression and reversed cyclic shear (Hiotakis 2004), and a full RC building subjected to seismic loading (Nagae et al. 2011a, 2011b, and 2015) are analysed using the proposed finite element material model. For each example, the validation is done following three steps. First, a description of the test is made, followed by theoretical analysis using the Mazars material model, where the analysis method is explained, finishing with a comparison of the theoretical results with the experimental results.

CHAPTER 2 – BACKGROUND AND LITERATURE REVIEW

This chapter presents a literature review and discussion on typical mechanical properties of concrete under uniaxial and biaxial states of stress. These properties are essential for the development of a numerical model for concrete. A description of two of the most important approaches for describing the behaviour of concrete uniaxial and biaxial behaviour is presented. A discussion of three state-of-the-art, finite-element programs that are widely used by practicing engineers and researchers to model reinforced-concrete structures is presented.

2.1 Introduction

Concrete is a composite material, made of inert granular aggregates joined by a paste of hydrated cement. Its complex structure gives concrete a non-homogeneous behaviour that depends in several factors, such as the design constituents, water-cement ratio, mixing, placement and curing conditions (Li, 2011). When the aggregate is mixed with cement and water, the mixture reacts chemically to create a hard matrix that binds the materials together into a durable material. Being a non-homogeneous material causes the concrete to contain a large number of micro-cracks, especially at the interfaces between the coarser aggregates and the cement paste, even at low levels of loading (Hsu and Mo, 2010).

The propagation of microcracks during the loading phase contributes to the nonlinear behaviour of concrete at low stress level as well as near failure. Some of these microcracks are caused by segregation, shrinkage and thermal expansion in the cement (Hsu and Mo,

2010). The rest of them are developed during loading, because of the differences in the stiffness between the aggregates and cement. The difference in stiffness can create strains in the interface zone several times larger than the average strain presented in the composite system. Since the interface of the aggregate-cement matrix has a significantly lower tensile strength than cement, it constitutes the weakest link in the composite system (Karsan and Jirsa, 1969). The composite structure of concrete generates a highly nonlinear behaviour in the material. The properties of concrete under uniaxial loading need to be studied, as well as the biaxial properties, in order to generate the correct element formulations for each case.

2.2 Uniaxial Behaviour of Concrete

A typical stress-strain relationship for concrete subjected to uniaxial compression and tension is shown in Fig. 2.1. The behaviour of concrete under compression is very different from the tensile behaviour, due to the composite structure of the material. Karsan and Jirsa (1969) described the uniaxial compressive stress-strain curve of concrete, as having a nearly linear-elastic behaviour up to about 30 percent of its maximum compressive strength, f'_c . For stresses above this point, the curve shows a gradual increase in curvature up to about $0.75 f'_c$, where it bends more sharply as it approaches the peak point, f'_c . Beyond the peak stress, the stress-strain curve has a descending branch until the concrete crushes, which occurs at the ultimate strain ϵ_u . In tension, the stress-strain curve is nearly linear-elastic up to the cracking stress, f_t . After this point in tension, plain concrete cracks and loses its capacity to carry any more tensile load.

The shape of the stress-strain curve is closely associated with the mechanism of internal progressive micro-cracking. For a stress in the linear-elastic region, the amount and size of the cracks existing in concrete before loading remain nearly unchanged. In compression, a stress level of about 30 percent of f'_c has been proposed as the limit of the elastic behaviour of concrete. On the other hand, the tensile stress-strain relationship is assumed to be elastic before the cracking strength. In compression, for stresses between 30 to 75 percent of f'_c , the micro-cracks in the cement-aggregate interface start to extend to the actual cement paste. If the load is reversed while the material is in the stress range between 30 and 75 percent of f'_c , the unloading and reloading path will follow closely the initial loading path.

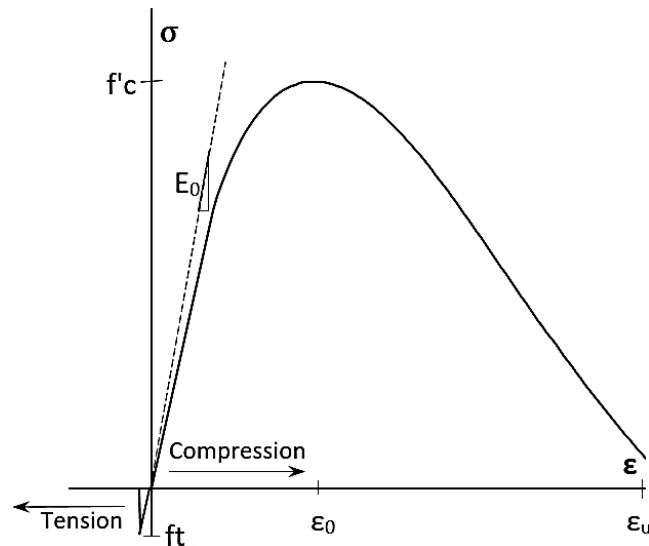


Figure 2.1. Typical plot of stress vs. axial strain

However, for unloading from stress at and over about 75 percent of f'_c , the unloading and reloading curves exhibit strong nonlinearities, showing a significant degradation of the stiffness and the presence of residual (plastic) strains in the material.

The degradation in both stiffness and strength for plain concrete under an increasing number of compressive load cycles is presented in Fig. 2.2. Each hysteresis loop corresponds to one cycle of unloading and reloading. It is seen that the stress-strain curve for monotonic loading (the broken line in Fig. 2.2) serves as an envelope for the peak values of stress for concrete under cyclic loading.

The progressive damage of concrete near f'_c is primarily caused by microcracks through the cement, and these form microcrack zones or internal damage. At this point the material has reached its maximum compressive strength, but compressive strain can be applied still. With the increase of the compressive strain, damage to the concrete material continues to accumulate, and the concrete enters the descending portion of its stress-strain curve, a region marked by the appearance of macro-cracks (Karsan and Jirsa, 1969).

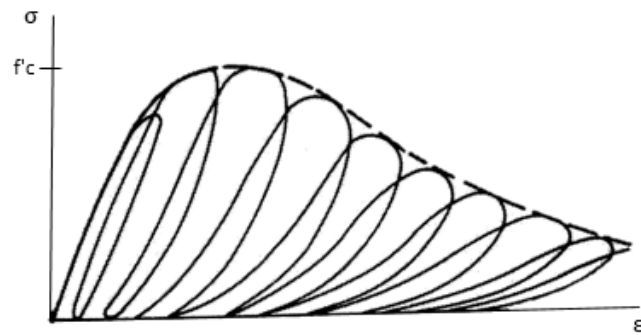


Figure 2.2. Uniaxial compressive response with unloading and reloading paths at different strains (Hsu and Mo, 2010)

The shape of the stress-strain curve is similar for concrete of low, normal and high strength, as shown in Fig. 2.3. A high strength concrete behaves nearly elastically in compression up to a relatively higher stress level than that of low strength concrete (Wischers, 1978). On the descending portion of the stress-strain curve, higher strength concrete tends to

behave in a more brittle manner, with the stress dropping off more sharply than it does for concrete with lower strength, due to the increase of the speed in the development of cracks in the material. The initial modulus of elasticity of concrete increases with the increase of the maximum compressive strength of the concrete (Wischers, 1978).

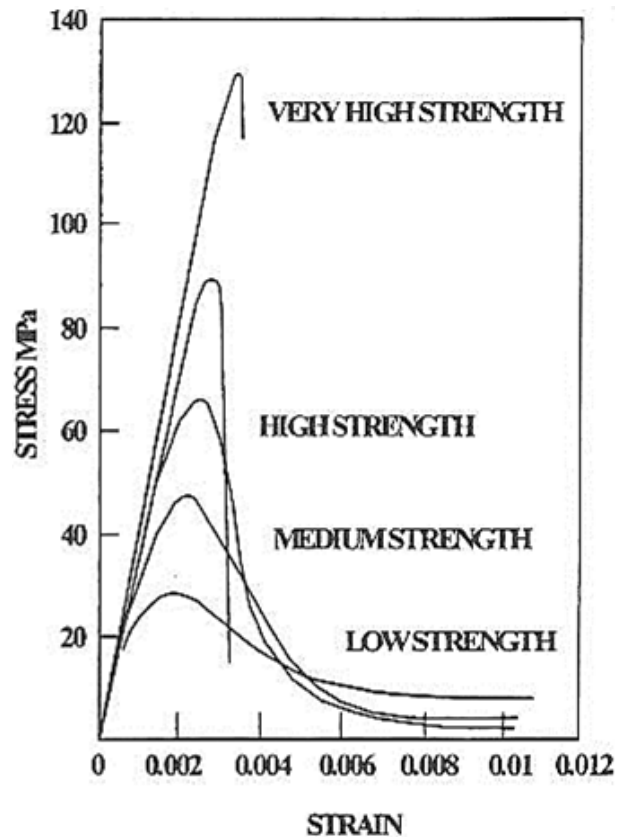


Figure 2.3. Compressive stress-strain curve for different concrete strengths (Attard et al., 1986)

2.3 Uniaxial Concrete Models

There are different material models that attempt to describe the uniaxial and the biaxial behaviours of concrete. Analytical models for the full stress-strain relationship of concrete in compression and tension are required for the numerical simulation of the structural behaviour of reinforced concrete structural elements. These models are generally

empirical, and based on tests conducted either on plain concrete specimens or on reinforced concrete ones.

2.3.1 Hognestad Model

One of the earliest and simplest models for compression in concrete with a nonlinear behaviour is the so-called Hognestad model for uniaxial compression of concrete (Hognestad, 1951). The model describes the inelastic behaviour of concrete as a parabola, which can be defined using two values: the concrete strength and the strain at which the concrete achieves its peak strength.

The stress-strain curve for the Hognestad model is given by:

$$f_c = f'_c \left[\frac{2\varepsilon_c}{\varepsilon_{c0}} - \left(\frac{\varepsilon_c}{\varepsilon_{c0}} \right)^2 \right] \quad 0 \leq \varepsilon_c \leq 2\varepsilon_{c0} \quad (2.1)$$

Equation 2.1 relates the stress f_c with the strain at the given state ε_c , where f'_c is the maximum compressive strength of the concrete, and ε_{c0} is the corresponding strain.

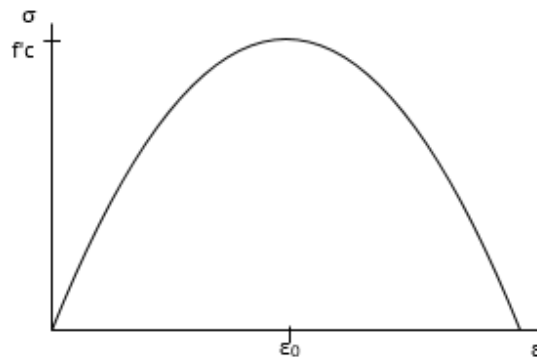


Figure 2.4. Compressive stress-strain curve (Hognestad, 1951)

Figure 2.4 shows the complete stress-strain curve for concrete under uniaxial compression according to the Hognestad model. The model accurately represents the ascending branch

of the actual concrete behaviour, but the descending branch is a mirror of the ascending part, which is not the case for the real behaviour of concrete.

2.3.2 Kent and Park Model

Kent and Park (1971) proposed a stress-strain equation for both unconfined and confined concrete. In their model, they generalized Hognestad's (1951) equation to better describe the post-peak stress-strain behaviour. The ascending branch is given by the following equation:

$$f_c = f'_c \left[\frac{2\varepsilon_c}{\varepsilon_{c0}} - \left(\frac{\varepsilon_c}{\varepsilon_{c0}} \right)^2 \right] \quad 0 \leq \varepsilon_c \leq \varepsilon_{c0} \quad (2.2)$$

The post-peak branch was assumed to be a straight line whose slope was define primarily as a function of concrete strength, f'_c .

$$f_c = f'_c [1 - Z(\varepsilon_c - \varepsilon_{c0})] \quad \varepsilon_{c0} \leq \varepsilon_c \leq \varepsilon_u \quad (2.3)$$

In which,

$$Z = \frac{0.5}{\varepsilon_{50u} - \varepsilon_{c0}} \quad (2.4)$$

Where, ε_u is the strain at which the concrete crushes, and ε_{50u} is the strain corresponding to the stress equal to 50% of the maximum concrete strength.

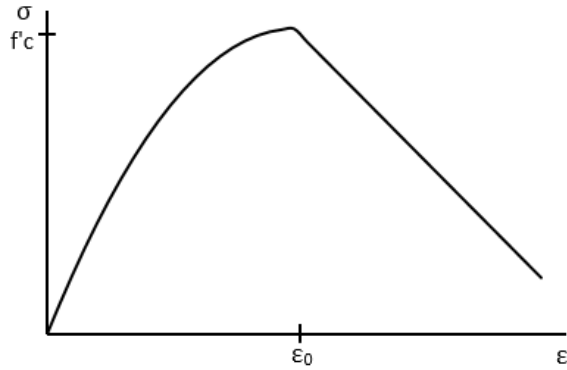


Figure 2.5. Compressive stress-strain curve from Kent and Park (1971)

Figure 2.5 shows the complete stress-strain curve for concrete under uniaxial compression as described by the Kent and Park model for concrete. This curve resembles the behaviour of concrete more accurately, even in the post-peak branch. Kent and Park's model is still widely used by the engineering community because of its simplicity. It is also widely used in finite-element modelling of concrete structures.

2.3.3 Tensile Model for Concrete

Tensile behaviour in concrete is often neglected in uniaxial models as a conservative measure, but it is important in the case of reinforced concrete. The tensile behaviour of concrete can be described as an elastic material before reaching its cracking strength. After reaching cracking, concrete abruptly loses its capacity to carry load.

$$f_c = E_c * \varepsilon_c \quad 0 \leq f_c \leq f_t \quad (2.5)$$

Where f_c is the stress in the concrete in tension, ε_c is the strain at the given state, f_t is the cracking strength of the concrete (usually between 8 and 12 percent of the maximum compressive strength), and E_c is the initial elastic modulus of the concrete (Fig. 2.6).

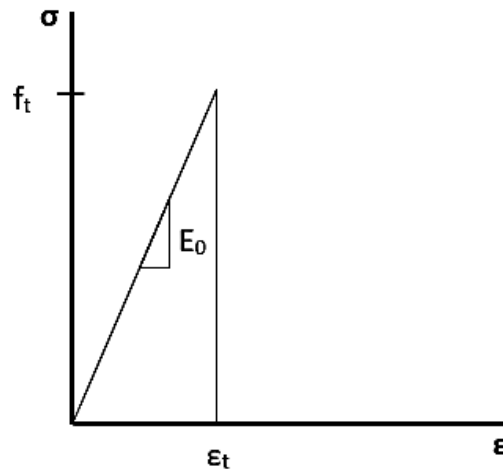


Figure 2.6. Tensile stress-strain relationship of concrete

2.4 Biaxial Behaviour of Concrete

The behaviour of concrete when subjected to a biaxial state of stress is of importance when the resistance and deformation of elements such as shear walls, deep beams and slabs needs to be predicted. In recent years, a large amount of research has been done on the mechanical properties of concrete under biaxial loading. Figure 2.7 shows the failure envelope for a concrete element subjected to a biaxial state of stresses.

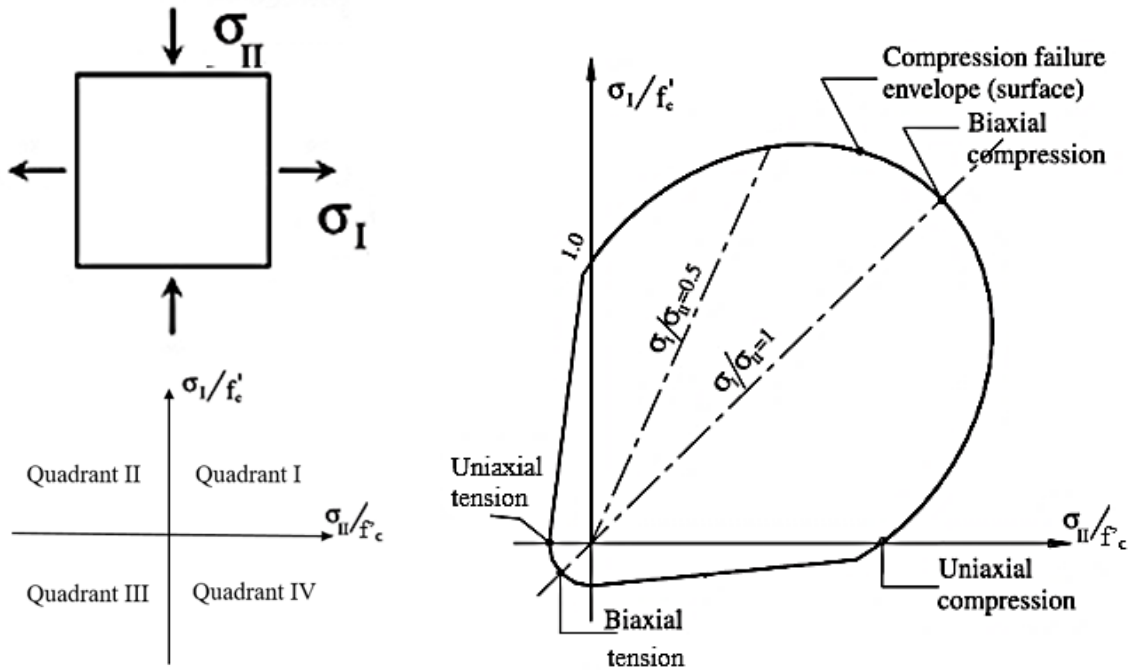


Figure 2.7. Biaxial behaviour of concrete (Ebead and Neale, 2005)

Each point of the failure envelope in Fig. 2.7 is calculated increasing the stresses at the same ratio in the element until failure. The following differences from uniaxial behaviour are to be noted.

- The maximum compressive strength increases for the biaxial - compression state (Quadrant I). A maximum strength increase of approximately 25 percent is achieved at a stress ratio of $\sigma_I/\sigma_{II}=0.5$, and an increase of about 16 percent is achieved at an equal biaxial-compression state ($\sigma_I/\sigma_{II}=1.0$). Under biaxial compression-tension (Quadrants II and IV), the compressive strength decreases almost linearly as the applied tensile stress is increased, this phenomenon is known as compression softening. Under biaxial tension (Quadrant III), the strength is approximately 20 percent smaller than that of uniaxial tensile strength.

- Failure of concrete occurs by tensile splitting with the fracture surface orthogonal to the direction of the maximum tensile strain. Tensile strains are of crucial importance in the failure criterion and failure mechanism of concrete. The failure of concrete under all combinations of biaxial loading appears to be based on a maximum-tensile-strain criterion (Tasuji et al. 1978). The interaction in the axial and transverse strains in the concrete element can be explained using the Poisson's ratio ν . The Poisson's ratio ν for concrete ranges from about 0.15 to 0.22.

2.5 Biaxial Concrete Models

The necessity of predicting the performance of concrete under biaxial loading has led to the development of several analytical biaxial concrete models. These can be divided in two major categories: Total-strain models, and Damage-based models.

2.5.1 Total-Strain Models

A total-strain model describes the average element stresses as a function of the average strains using the constitutive models from the materials. This type of models can use either principal strains or global strains. When global strains are used, the interaction of the normal and shear strains must be taken into account. This is usually done by introducing an empirical ratio depending on the model used. The constitutive relationships and compatibility of strains are dependant in both the behaviours of concrete and steel.

Examples of these models are the Modified Compression Field Theory (Vecchio and Collins, 1986), and the Cyclic Softened Membrane Model (Mansour and Hsu, 2005).

2.5.1.1 Stress Condition and Crack Pattern

A reinforced-concrete, 2-D element subjected to in-plane shear and normal stresses can be separated into a concrete element and a steel grid element (Fig. 2.8).

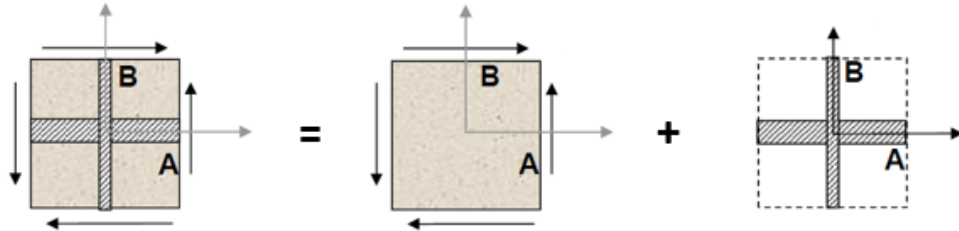


Figure 2.8. Decomposition of a RC element

Before cracking, the principal stresses in the concrete element coincide with the applied principal stresses in the RC element, while after cracking, the direction of the subsequent cracks deviate from the direction of the first crack, as seen in Fig. 2.9. In view of the fact that the angle of subsequent cracks occurs between the angle of the principal applied stresses and the angle of the principal concrete stresses, two types of theories have been developed: rotating angle shear theories, and fixed angle shear theories.

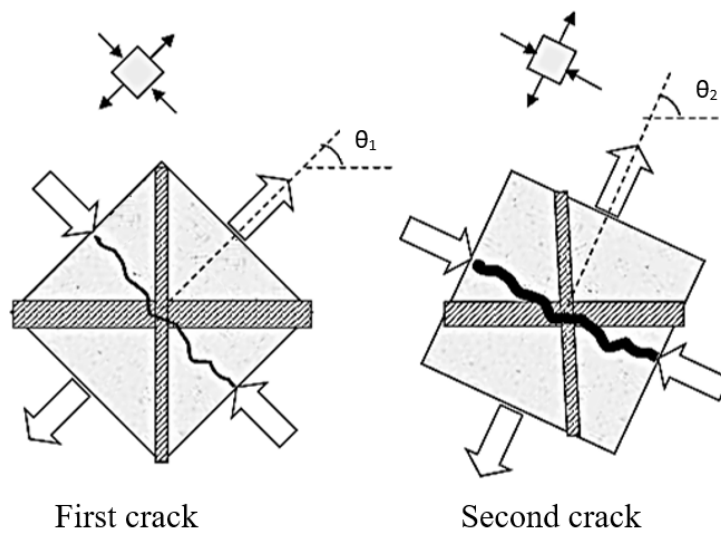


Figure 2.9. Change in subsequent crack angles

2.5.1.2 Rotating Angle Shear Theories

The Rotating Angle Shear Theories are based on the orientation of the concrete principal stresses. As the stresses applied to the element increase, the concrete element cracks, and the angle of the principal stresses in the concrete element deviates from the principal applied stresses. Therefore, this type of theory is called a “rotating angle” one. The constitutive relationships for rotating angle models are developed in terms of the direction of the principal stresses in the concrete element, thus avoiding the need to explicitly consider the effect of shear stresses. This is because the shear stress vanishes at the orientation of the principal stresses in the concrete element. One of the most prominent rotating angle theories is the Modified Compression Field Theory (Vecchio and Collins, 1986), a model that is the base of the General Method for shear design in the Canadian code for concrete structures (CSA A23.3-14).

2.5.1.3 Modified Compression Field Theory (MCFT)

Vecchio and Collins (1982) proposed the Compression Field Theory (CFT), which is based on the rotating angle approach. In this model, the directions of orthotropy are taken normal and parallel to the direction of the principal strain and are continuously changed during loading. The CFT neglects the contribution of concrete to tension because the tensile strength of concrete is assumed to be zero. As a result, the CFT is able to predict failure loads but cannot accurately predict the deflections under shear. In 1986, the CFT was revised to develop the Modified Compression Field Theory (Vecchio and Collins, 1986),

by including a relationship for concrete in tension to better model the deformation of the elements when subjected to shear stresses.

In the MCFT, the cracked reinforced concrete is treated again as an orthotropic material with its principal axes in the direction of the principal strains. The Poisson's effect is neglected after the cracking of concrete, considering that after cracking the axial deformations do not affect the transverse deformations. Equilibrium between the internal and external forces can be achieved with an iterative procedure such as a Newton-Raphson technique using a secant stiffness matrix approach (Vecchio and Collins, 1986).

Figure 2.10 shows the summary of the MCFT for the analysis of reinforced concrete 2-D panels. The implementation of the model is briefly described next for completeness. Equations 2.6 to 2.10 show the equilibrium of forces in a generic panel, that relates the applied stresses to those in the concrete and steel materials. Equations 2.11 to 2.13 illustrate relationships among the strains are distributed in the rotated cracked concrete element. Equations 2.14 and 2.15 relate the crack widths in the concrete element with the spacing of the steel reinforcement and the principal tensile strain. Equations 2.16 to 2.19 are the material constitutive relationships, which include the tensile response of the concrete in Eq. 2.19 as the principal improvement over the CFT.

The MCFT builds the constitutive relationship in terms of principal strains thereby avoiding the necessity of building a constitutive model for shear, but including a separate equation that checks concrete shear stress on crack surfaces, shown in Eq. 2.20.

Characterizing the behaviour of a generic, reinforced concrete element requires the simultaneous solution of the 15x15 nonlinear system of equations described in Fig. 2.10.

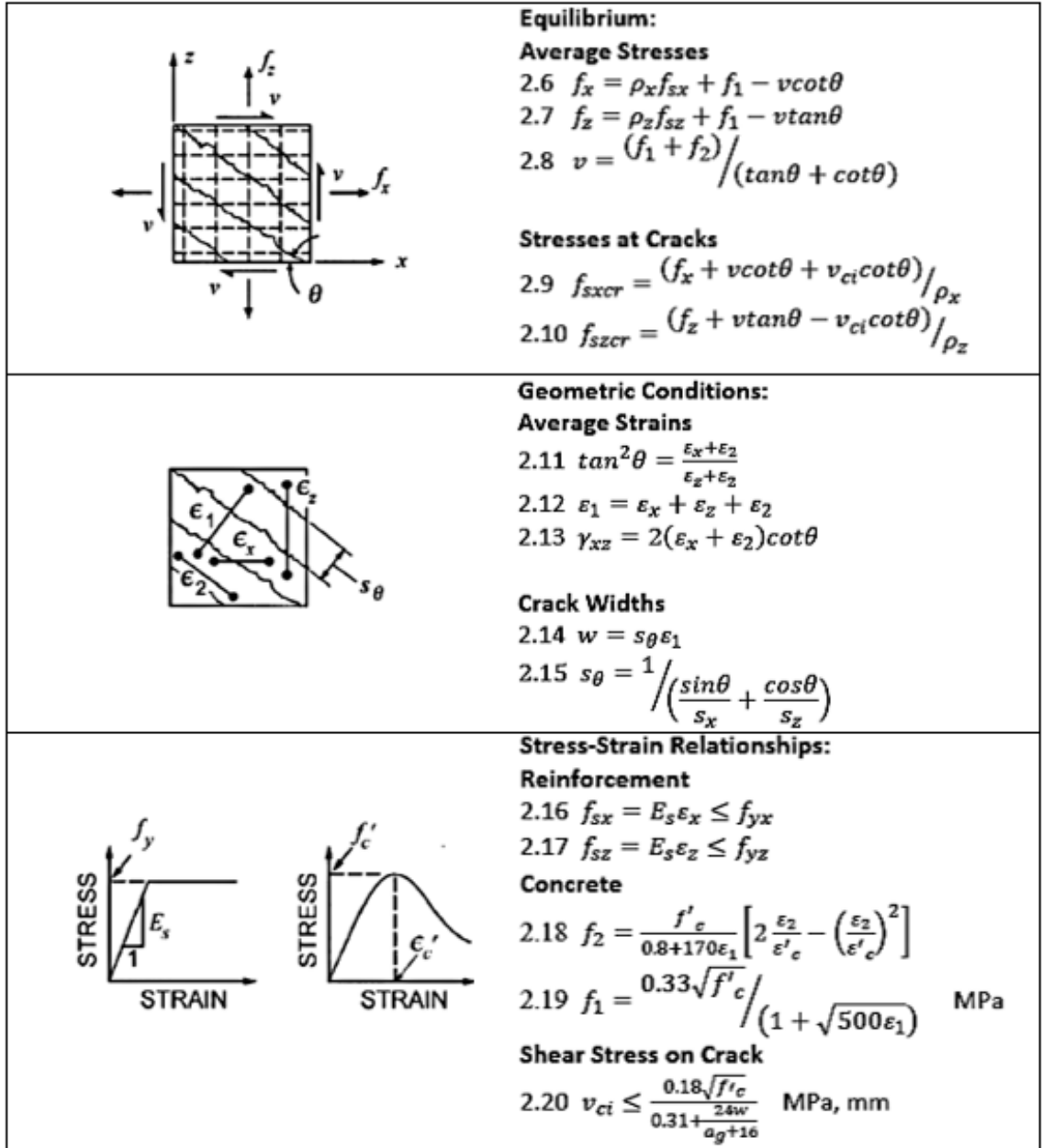


Figure 2.10. Summary of MCFT for reinforced concrete (Vecchio and Collins, 1986)

2.5.1.4 Fixed Angle Shear Theories

The Fixed Angle Shear Theories are based on the orientation of the applied principal stresses in the RC element, which never changes during the application of load if the

applied stresses are increased proportionally. A fixed crack model allows a deviation between principal applied stresses in the RC element and principal stresses in the concrete element. This deviation creates a need to relate the shear stresses in the element with the normal stresses, affecting the overall element performance.

2.5.1.5 Cyclic Softened Membrane Model (CSMM)

The Cyclic Softened Membrane Model (Mansour and Hsu, 2005) was developed based on the Fixed-Angle Softened Truss Model (Pang and Hsu, 1996). This model predicts the reversed cyclic shear response of reinforced concrete membrane elements using a fixed crack approach, including different constitutive models for concrete and steel that include unloading and reloading effects.

Similarly, as in the case of the MCFT, enforcing equilibrium between external and internal forces using this method necessitates an iterative procedure such as the Newton-Raphson solution scheme, using a tangent stiffness matrix approach. Figure 2.11 shows the summary of the CSMM for the analysis of reinforced concrete 2-D panels. The way that the CSMM models the different materials in a reinforced concrete element is briefly described next, using Fig. 2.11.

Steel. The uniaxial material constitutive model for steel considers the stress-strain response of a steel rebar considering the presence of the surrounding concrete. It is seen that the behaviour on an embedded bar is different from the bilinear response of bare steel, as observed in the constitutive model for steel in Fig. 2.11. This is due to the transfer of tensile stresses that occur between the steel and the concrete.

Concrete. The concrete constitutive model includes the softening effect produced by the strains in the perpendicular direction to that being analysed, as well as the smooth decrease in the tensile stress after cracking. The cyclic constitutive laws of concrete and steel bars are used in the CSMM, including plastic strains in their formulations.

The CSMM determines equivalent uniaxial strains to define compressive and tensile constitutive relationships. The shear stress is expressed as a function of the corresponding axial strains and stresses in the principal directions, through the Hsu/Zhu ratios defined in Fig. 2.11. The Hsu/Zhu ratios were developed to include the additional concrete “growth” effect under proportional biaxial tension-compression loading, and to transform the bidimensional tensor of strains into their equivalent uniaxial strains for either concrete or steel.

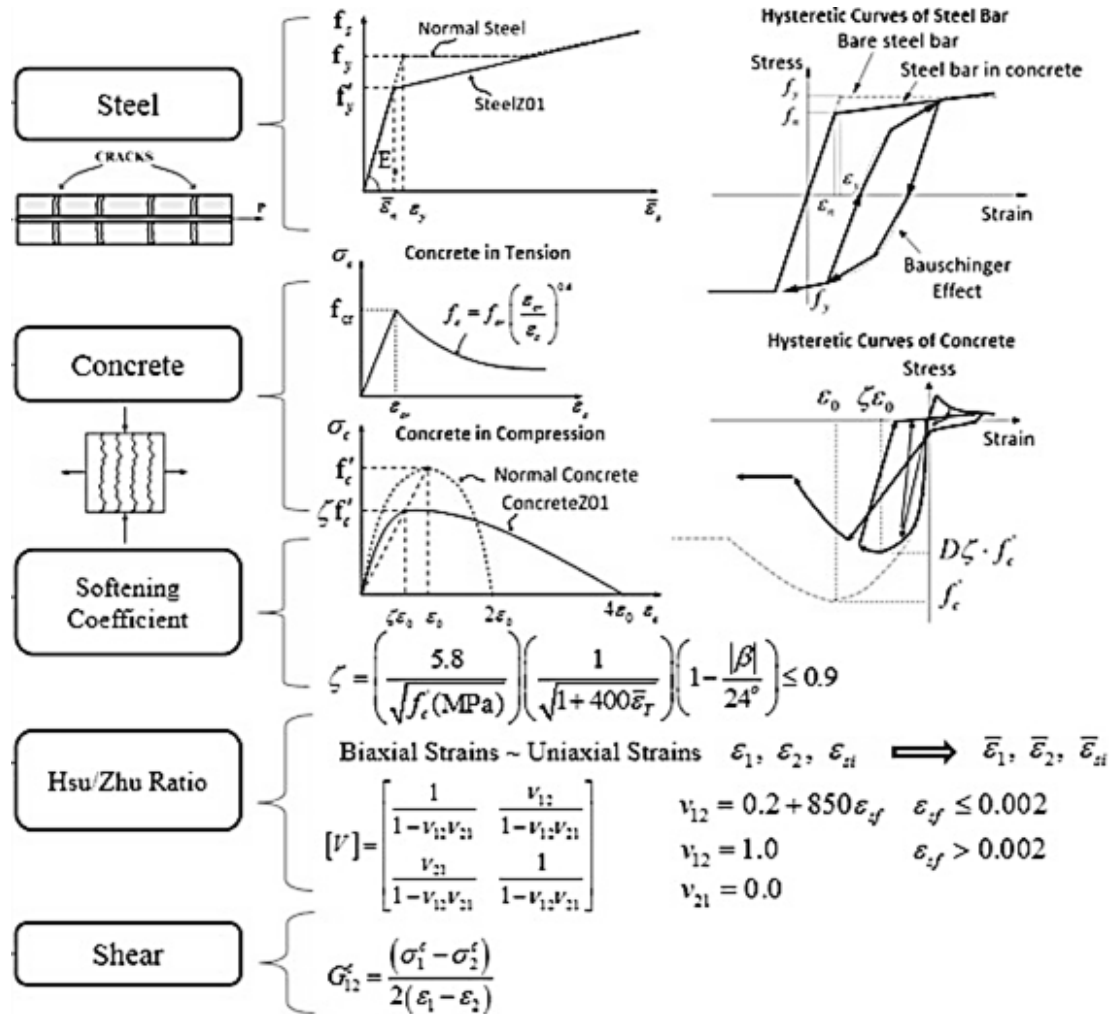


Figure 2.11. Summary of CSMM for reinforced concrete (adapted from Mansour and Hsu, 2005)

2.5.2 Damage-Based Models

Continuum damage mechanics was originally formulated as a tool to obtain a physical description of the internal failures that a material can exhibit. It was developed to describe different types of effects such as creep, fatigue, constant load and chemical reactions (Kachanov, 1958). It later evolved into an approach to describe material behaviour (Lemaitre, 1992). When applied to concrete, it is assumed that concrete is an isotropic material with a varying stiffness. The variation of the stiffness in the material is provided

by a scalar damage variable D , which is inversely proportional to the initial, elastic stiffness matrix of the material. The more damaged the material, the greater the value of the scalar damage parameter. A complete discussion of Damage-Based Models, as applied to concrete, is given in Chapter 3.

2.6 Structural Simulation Using the Finite Element (FE) Method

In the last years, the FE method has become an important tool for the analysis of reinforced concrete structures, and many material constitutive relationships, element formulations and solution schemes have been developed for the use in FEA. Continuous improvement of nonlinear finite element techniques and computing facilities make the simulations of reinforced concrete structures more feasible.

In research-oriented analysis of RC structures, the implementation of concrete and RC material models have led to the development of specialized finite element software that has been proven to lead to accurate simulations of the nonlinear behaviour of shear wall specimens (Lee and Kuchma, 2007; Han et al. 2010; Zhang and Li, 2012; Ali et al. 2013; Luu et al. 2013; Mergos and Beyer, 2013; Genikomsou and Polak, 2014). However, these research-oriented tools have at least one of the following three limitations, or a combination of them: a) either their source-code is proprietary, which makes difficult for researchers to implement the latest research results on shear wall behaviour or verify the theory behind the code, b) the number of elements and nodes that they can handle are insufficient to model complete structures, which drastically reduces their usefulness, and c) the more accurate and advanced the material model implemented in the software, the greater the possibility of occurrence of convergence and numerical problems in large models. Due to

the combination of these factors, finite-element simulations of complete shear wall structures (at the system level) are very scarce.

The capabilities of currently available FE software to predict the behaviour of shear wall structures (at the component and system levels), are briefly described next.

2.6.1 Abaqus FEA

Abaqus FEA is a suite of general-purpose software applications for finite element analysis and computer-aided engineering design. Users can implement their own nonlinear material models via user material subroutines (Abaqus, 2009). Three different constitutive concrete models are available in Abaqus: the smeared crack concrete model, the brittle cracking model, and the concrete damaged plasticity model.

The smeared crack concrete model is an elasto-plastic model controlled by a “compression” yield surface. Cracking is assumed to be the most important of the behaviour of the material. This material model is intended for applications in which the concrete is exclusively subjected to monotonic loading. The brittle cracking model is useful in applications where the failure of concrete is given by tensile cracking. The behaviour in compression is assumed to be elastic, making it not suitable for any kind of dynamic analysis with load reversals. The concrete damaged plasticity model is damage-based material model, that can be used in applications where the concrete is subjected to any kind of loading conditions, including cyclic loading (Abaqus 2009).

Studies on the response of RC elements using Abaqus have focused mainly on response at the component level. The behaviour of a RC beam element under the effect of impact

vibration was studied using the concrete damaged plasticity model, generating several models with different mesh sizes, damping values, and compression and tension stiffness recovery, to better represent the test results (Ahmed, 2014). The investigation of punching shear in RC flat slabs without shear reinforcement, using the same concrete model in 3D elements, relating the results obtained for ultimate load, deflections and cracking patterns with these results (Genikomsou and Polak, 2014). Studies on the seismic response of complete reinforced concrete structures using Abaqus are scarce. Zhang and Li (2012) tested a 1/5 scale-three story frame and shear wall RC structure under the 'El Centro' earthquake, and compared the results with an Abaqus model. The FEA model consisted on fiber elements for columns and beams, and shell elements for slabs and shear walls, the material properties were introduced as user-defined dynamic material subroutines. The FEA results were in accordance of the experimental results when considering the strain rate effect in the material. Han et al (2010) studied the crack development, failure pattern and the displacement ductility of a prestressed precast RC frame under cyclic loading, using a FEA model with solid 3D elements for concrete, linear-truss elements for the reinforcing and prestressed steel. The skeleton curves of the hysteresis loops of both the test and the FEA model, presented very similar behaviours for the frame. Ali et al (2013) studied the nonlinear cyclic behaviour of shear walls with composite steel-concrete. Concrete damaged plasticity material was used in solid 3D elements and subjected to a cyclic loading program. The predicted load vs. deformation curves, peak loads, ultimate strength values and deformation profiles showed good agreement with experimental skeleton curves.

Abaqus FEA shows accurate results when studying the performance of an element or a structure under different types of loadings. Abaqus provides a reasonable user-interface and access to some subroutines. However, the source-code is proprietary, which makes difficult for researchers to implement the latest results or to verify the theory behind the code. Also, limiting the solution algorithms to the ones contained in the software, which may not be suitable to obtain a solution without convergence problems. This makes it impossible to analyze engineering phenomena not considered before, or to analyze the behavior of a newly-found material.

2.6.2 VecTor2

VecTor2 is a nonlinear finite element analysis program for the analysis of 2-dimensional RC membrane structures. VecTor2 uses a smeared, rotating-crack formulation based on the MCFT (Vecchio and Collins, 1986) and the Disturbed Stress Field Model (DSFM) (Vecchio, 2000). A wide range of material constitutive models are available for representing the material responses and mechanisms of reinforced concrete structures. VecTor2 contains 25 concrete material types and 25 steel material types (smeared reinforcement and truss reinforcement), for the use in the analysis of 2D RC structures, using four-node quadrilateral elements (Wong et al. 2013).

The program gives accurate results when modelling RC shear wall, or 2-dimensional structures. The seismic overstrength of shear walls of parking structures was investigated by inelastic static pushover analyses and inelastic dynamic response analysis (Lee and Kuchma, 2007). The results obtained in FEA resembled closely the test results. Two series of shake table tests on slender RC walls were analysed using VecTor2 (Luu et al. 2013).

Damping was assumed to be 1.5% for the wall, and the model was able to predict the natural periods of the walls in elastic and damaged conditions. The FEA model was able to predict the crack pattern, as well, showing the damage response of the actual test. Quasi-static tests on RC walls were compared with FEA model using VecTor2 (Mergos and Beyer, 2013). The shear-flexure interaction response of the tall walls in the FEA model resembled very closely the test results selected to validate the model.

However, VecTor2 cannot perform analyses in a 3D environment, nor can it be used to model a full structure due to the small number of elements allowed by the program (6000 elements, 5200 nodes). This makes it not suitable for the analysis at the system level of a RC structure. On the other hand, VecTor2 does not allow the modification or addition of new analysis modules to its source code.

2.6.3 OpenSees

OpenSees stands for Open System for Earthquake Engineering Simulation, and was developed at the Pacific Earthquake Engineering Center (PEER), University of California, Berkeley. OpenSees is an object-oriented, open-source framework for simulating applications in earthquake engineering using finite element methods (Fenves, 2001). The behaviour of structural and geotechnical systems can be simulated in OpenSees using a modular approach, this means that the model configuration, numerical solution, and output recorder are independently defined.

The flexibility of this modular implementation enables OpenSees to be enhanced in an open-source fashion in which new components, such as material models, element types,

and analysis formulations, can be included as they are developed. Key features of OpenSees include the interchangeability of components and the ability to integrate existing libraries and new components into the framework without the need to change the existing code (Fenves, 2001).

Many advanced finite element techniques that are suitable for the nonlinear finite element analysis have already been implemented in OpenSees. A damage-based concrete material model has been implemented (Lu et al. 2015) in the OpenSees framework (Fenves, 2001), which can be used in multilayer-shell elements to simulate the behaviour of reinforced concrete plane stress structures. A biaxial concrete material model based on the CSMM has been implemented (Zhong, 2005) in OpenSees, which has shown to accurately predict the behaviour of shear walls when subjected to reversed-cyclic loading. However, research groups that develop biaxial concrete materials for this framework usually make their source code proprietary and thus key aspects of their performance are unknown.

CHAPTER 3 – DAMAGE MODEL FOR CONCRETE

This chapter describes the material model to be implemented for the analysis of concrete under bidimensional loading. Generalities, definitions and theoretical framework for Damage Based Models are presented first, followed by the description of the Mazars Concrete Damage Model. Parametric analyses investigating the influence of the variables of the model on the concrete response are discussed and a number of numerical analyses of the biaxial response of simple structures are presented to verify the accuracy of the proposed algorithm. Then, the coordinate system, equilibrium and compatibility equations used in the Mazars model are described in a finite element formulation, resulting in a material constitutive matrix of concrete based on the Mazars model. The material constitutive matrix is presented in its secant formulation. Also presented is the implementation of the Mazars model for 2D plane stress elements into the finite element framework OpenSees (Fenves, 2001).

3.1 Introduction

Damage-based models for concrete are derived from continuum damage mechanics and adapted to describe the nonlinear behaviour of concrete. Continuum damage mechanics originally started as a physical description of the internal failures that a material can exhibit at the micro- and macro-scale, produced by different types of effects such as creep, fatigue, constant load and chemical reactions (Kachanov, 1958), defining the creation, propagation, and expansion of concrete microcracks as ‘damage’.

Concrete is a composite material composed by granulates in a brittle matrix (the hydrated cement paste). The change in the internal structure of the cement matrix, the interface between the cement matrix and the aggregate grains and with the voids in the structure, when subjected to loading, can be described by damage mechanics. The collapse of the structure of the cement matrix and the propagation of cracks are the reason why the stiffness of the concrete degrades under the action of loads. Describing the mechanical behaviour of concrete can be complex given the complexity of its microstructure, but using damage mechanics the behaviour of concrete can be simplified.

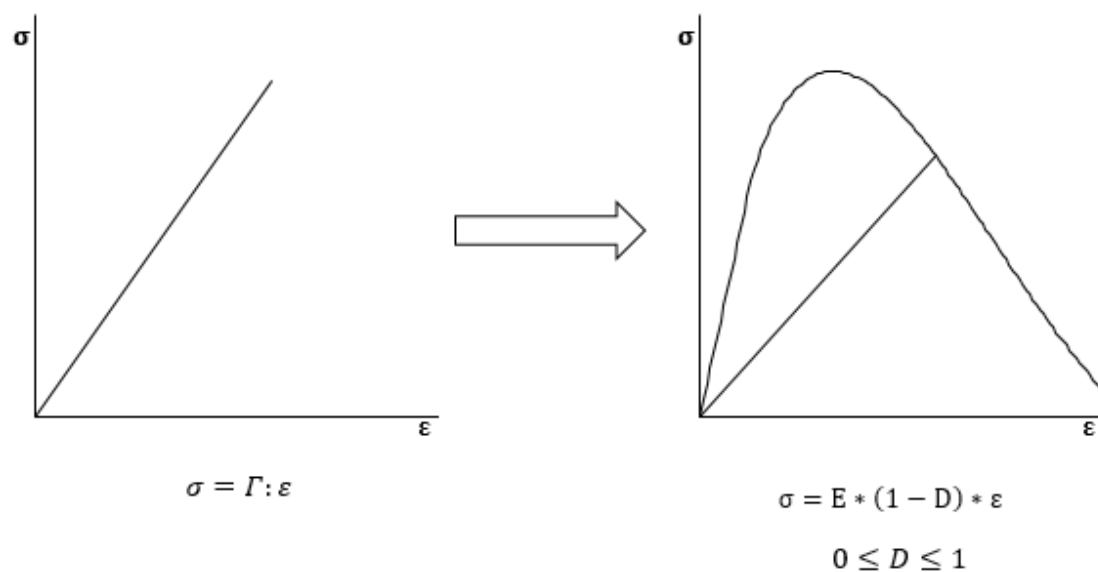


Figure 3.1. Elastic material vs. Damage material

Concrete damage models describe the behaviour of a material by assuming it is elastic with a constant stiffness. Upon being loaded, the stiffness is affected by a scalar damage parameter D , which ranges from 0 for the undamaged material to 1, which represents failure of the material (Fig. 3.1). Since the damage at any given point is considered to affect the material in every direction, the material is assumed to be isotropic. The element

formulations that control the behaviour of the damage variable D are derived from thermodynamic studies of the materials (Loland, 1980; Mazars, 1984), and its definition is dependent on the approach of each theory.

3.2 Mazars Model

Continuum damage mechanics is often used as a framework for describing the variations of the elastic properties of concrete due to micro-structural degradations (Lemaitre, 1992). Damage models in finite element analysis of concrete materials have been shown to successfully represent the behaviour of reinforced-concrete (RC) panels under in-plane loads (Mazars et al. 2002; Legeron et al. 2005; Mazars et al. 2015)

Mazars (1984) developed a scalar damage model describing the behaviour of the concrete as elastic-damageable. The model was developed to account for the triaxial behaviour of concrete. Isotropy is assumed. The model has a damage parameter given by an equivalent strain able to discriminate between tensile and compressive behaviour. It is a simple, robust model that relies in a scalar local variable D to describe the damage and reduction of the stiffness due to tensile and compressive damage separately.

Mazars' model explains the damage in concrete accounting for all the micro- and macro-effects of the loading, rearranging of the concrete particles, collapse of the micro-voids in the mixture, and the interaction of the cement matrix with the aggregates. This material model was created to represent the triaxial behaviour of concrete. The fact that all compressive strains can be represented by the tensile strains in the orthogonal directions,

makes it possible to simplify the element formulations and represent every deformation with tensile strains.

3.2.1 Analysis Procedure

A characteristic of this model is that the material constitutive, equilibrium and compatibility equations can be solved explicitly, and there is no need for an iterative procedure to obtain stresses when given an arbitrary set of strains. All the evolution laws for damage are expressed through an equivalent strain and a number of material parameters to describe the behaviour of the material under loading. These parameters make it possible to modify the shape of the calculated stress-strain concrete curve to represent the measured stress-strain relationship. The simplicity of the model makes its implementation in finite element analysis a straightforward process.

The stress is obtained assuming elastic behaviour in the material, with the presence of a scalar damage parameter D that ranges from 0 for the undamaged, “healthy” material, to 1, which represents failure of the material. Equation 3.1 relates the stress vector (σ) and the strain vector (ε), using the initial stiffness matrix (Γ) but multiplying it by the damage term ($1 - D$), obtained at the given state of the element.

$$\sigma = (1 - D)\Gamma : \varepsilon \quad (\Gamma: \text{Stiffness matrix}) \quad (3.1)$$

When the material is subjected to compressive loading, due to the presence of heterogeneities in the material (produced by the aggregates embedded into the cement matrix), tensile strains will generate a stress field orthogonal to the loading direction. Tensile strains generate micro- and macro-cracks in the concrete, which in turn generate

damage in the material. Thus, this theory is based on the assumption that every deformation can be described using tensile strains (Fig. 3.2). A state of deformation that includes normal and shear strains can be converted to a state of principal strains, leaving only normal compressive and tensile strains. Then, the compression in the element can be described with tensile strains in the orthogonal direction of the applied load.

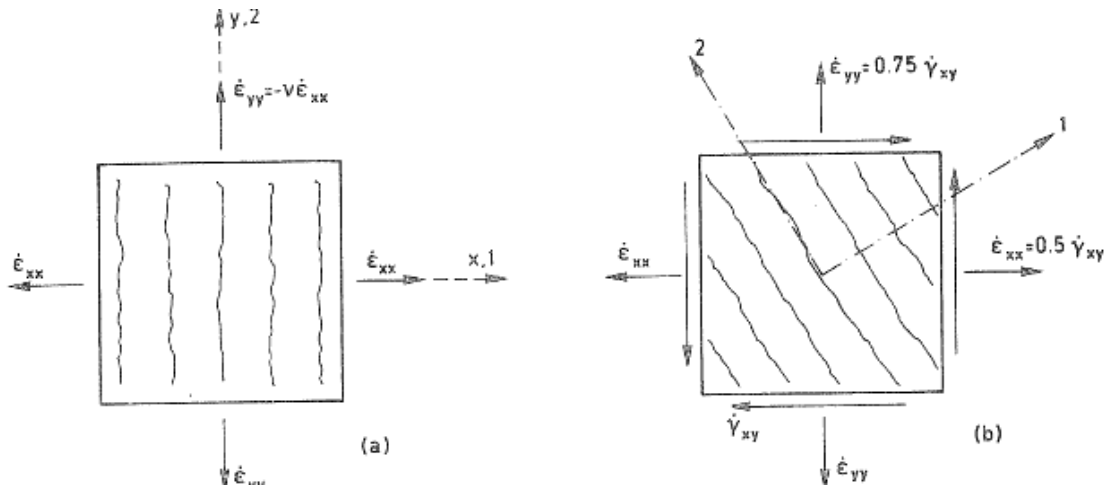


Figure 3.2. Use of tensile principal strains to describe any state of strains

The damage variable D is dependent on the tensile strains of the element, so an equivalent strain (ϵ_{eq}) is defined to make it possible to translate the triaxial state of strains to a uniaxial state of strain. The equivalent strain describes the amount of extension that the material is experiencing. Equation 3.2 calculates the equivalent strain (ϵ_{eq}) as the average of the tensile principal strains of the element. If a principal strain is compressive, it is not accounted in the calculation of ϵ_{eq} and it is taken as zero.

$$\epsilon_{eq} = \sqrt{\sum_{i=1}^3 (\langle \epsilon_i \rangle)^2}; \quad \text{where } \langle \epsilon_i \rangle = \epsilon_i \text{ if } \epsilon_i > 0 \quad (3.2)$$

$\epsilon_i = \text{principal strains, where } i = 1,2,3$

To differentiate the type of damage (compression or tension) to which the material is being subjected, the principal stress state (σ_p) is calculated with Eq. 3.2 and then divided in two tensors, one of them with only positive (tensile) stresses (σ_+), and the other with only negative (compressive) stresses (σ_-).

$$\sigma_p = (1 - D)\Gamma : \varepsilon_p \quad (3.3)$$

$$\sigma_p = \sigma_+ + \sigma_-$$

The tensile (ε_t) and compressive (ε_c) strain tensors are obtained from the tensors in Eq. 3.3 using the secant stiffness, as expressed by Eqs. 3.4 and 3.5.

$$\varepsilon_t = \left(\frac{1}{1-D} \right) \Gamma^{-1} : \sigma_+ \quad (3.4)$$

$$\varepsilon_c = \left(\frac{1}{1-D} \right) \Gamma^{-1} : \sigma_-; \quad (3.5)$$

The total damage of the element is defined as the weighted sum of the damage in tension and the damage in compression. The weights are obtained from the predominant response of each of the principal strains, defining the contribution of each type of damage (tensile or compressive) for general loading. Equations 3.6 and 3.7 define the weight of the tensile damage (α_t) and the weight of the compressive damage (α_c) respectively. These weights are a function of the principal strains due to either positive (tensile) or negative (compressive) stresses. Since the theory is based on the assumption that damage occurs via micro- and macro-cracking and that these cracks are generated exclusively from tensile strains, the weight exists only if the total strain (ε_i) is tensile. Therefore, the use of the H parameter, which is equal to 1 if the total strain is positive (tensile) or 0 if the total strain is negative (compressive).

$$\alpha_t = \sum_{i=1}^3 H_i \frac{\varepsilon_{ti}(\varepsilon_{ti} + \varepsilon_{ci})}{\varepsilon_{eq}^2} \quad (3.6)$$

$$\alpha_c = \sum_{i=1}^3 H_i \frac{\varepsilon_{ci}(\varepsilon_{ti} + \varepsilon_{ci})}{\varepsilon_{eq}^2} \quad (3.7)$$

where $H_i = 1$ if $\varepsilon_i = \varepsilon_{ci} + \varepsilon_{ti} \geq 0$, otherwise, $H_i = 0$, with $i = 1, 2, 3$

Since the model uses principal strains, there are only tensile and compressive stresses. Hence, one variable for the damage in tension (D_t) and another for the damage in compression (D_c) are needed. D_t and D_c are scalars that represent the mechanisms of deterioration sustained by the material in tension and compression, respectively. These variables reflect the irreversible damage that the material has accumulated. Their values are obtained using Eqs. 3.8 and 3.9.

$$D_t = 1 - \frac{\varepsilon_{D0} * (1 - A_t)}{\varepsilon_{eq}} - A_t * \exp[-B_t * (\varepsilon_{eq} - \varepsilon_{D0})] \quad (3.8)$$

$$D_c = 1 - \frac{\varepsilon_{D0} * (1 - A_c)}{\varepsilon_{eq}} - A_c * \exp[-B_c * (\varepsilon_{eq} - \varepsilon_{D0})] \quad (3.9)$$

Both types of damage depend on the initial damage threshold (ε_{D0}) and the equivalent strain of the element at that state (ε_{eq}), but D_t is related to the tensile material properties of the concrete (A_t, B_t) while D_c is related to the compressive material properties (A_c, B_c). The variables $\varepsilon_{D0}, A_t, B_t, A_c$ and B_c , modulate the shape of the tensile and compressive uniaxial curves, and they need to be adjusted to represent the actual material behaviour.

The initial damage threshold (ε_{D0}) is the strain at which the damage initiates. It affects the peak stress, but also the shape of the post-peak behaviour in both the tensile and compressive curves. In general, ε_{D0} ranges from 0.5×10^{-4} to 1.5×10^{-4} , and it can also be taken as the cracking strain of the concrete (ε_t). Before ε_{D0} , the behaviour of the material is

completely elastic, and after this threshold is surpassed A_t , B_t , A_c and B_c need to be adjusted to adjust the compressive and tensile curves of the material model with the stress-strain relationships obtained from compressive and tensile tests.

The variables A_t and B_t are the material parameters that reproduce the quasi brittle behaviour of concrete in tension. They need to be adjusted to represent the uniaxial tensile behaviour of concrete obtained from a direct tensile test or a split test.

A_t values are usually in between 0.7 to 1. Figure 3.3 shows the influence of A_t in the tensile response of concrete. As A_t increases, the damage given by tensile strains increases, eventually reaching complete damage at lower strains.

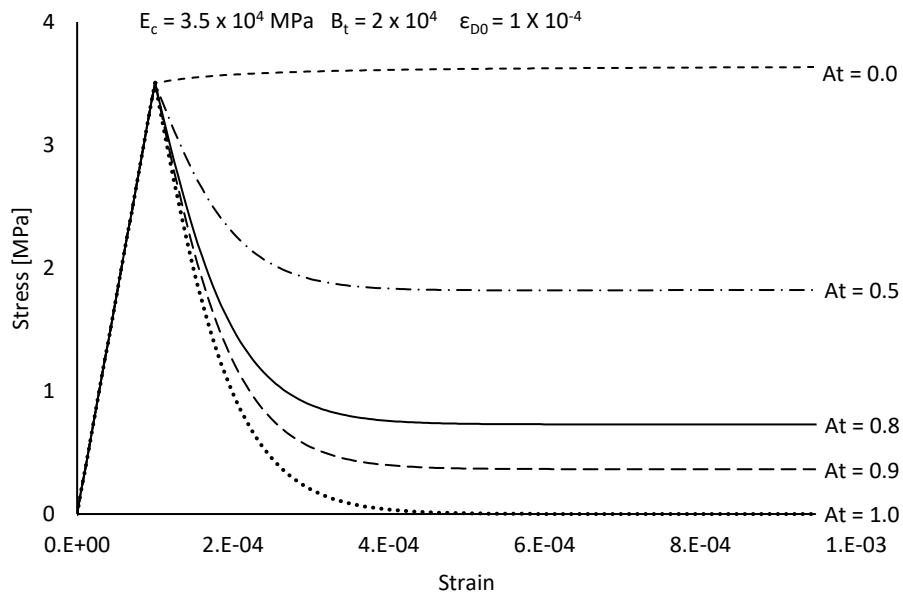


Figure 3.3. Influence of parameter A_t

The values of the parameter B_t usually range between 9,000 and 21,000. Figure 3.4 shows the influence of the B_t parameter on the tensile curve of the material. This parameter is the one responsible of describing the maximum tensile stress that the element can resist after

the damage threshold has been surpassed. As B_t decreases the maximum tensile stress that the material can reach is larger and presents at a higher strain.

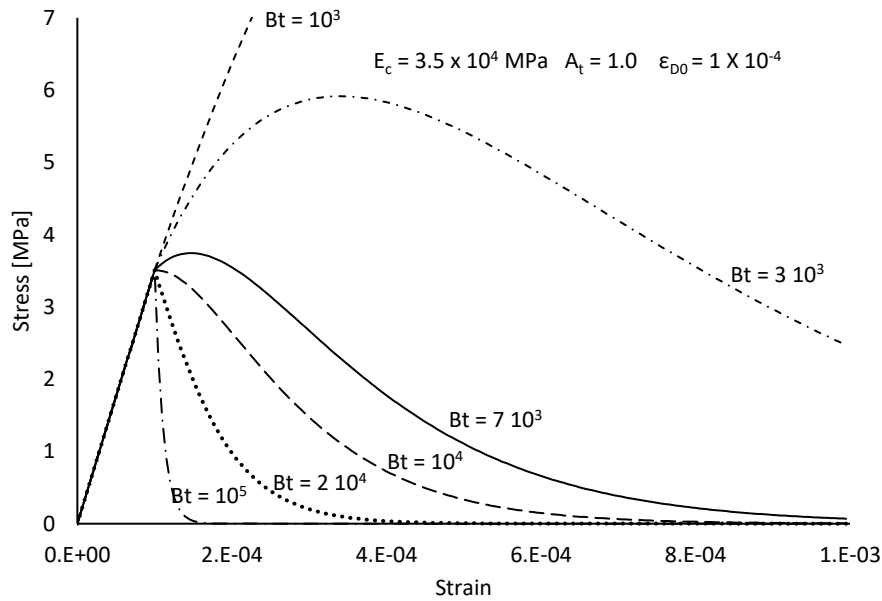


Figure 3.4. Influence of parameter B_t

The variables A_c and B_c are the material parameters that reproduce the compressive curve of concrete. They must be adjusted to represent the uniaxial compressive behaviour of concrete obtained from a compression cylinder test.

The values for the parameter A_c are usually between 1.0 and 2.0. Figure 3.5 shows the influence of the parameter A_c in the compressive response of concrete. A higher value of A_c will increase the maximum strength of the concrete and provide a steeper post-peak response, while decreasing the strain at which the damage will be equal to 1.

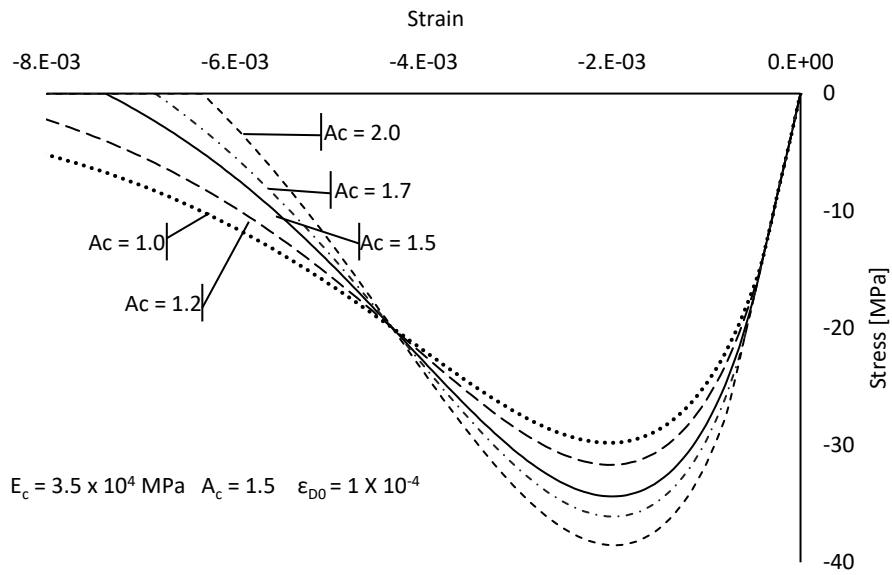


Figure 3.5. Influence of parameter A_c

The values of the parameter B_c usually range between 1,000 and 5,000. The parameter B_c is inversely proportional to the compressive strength and associated strain, as shown in Fig. 3.6. As the value of B_c increases, the maximum stress and its strain become smaller.

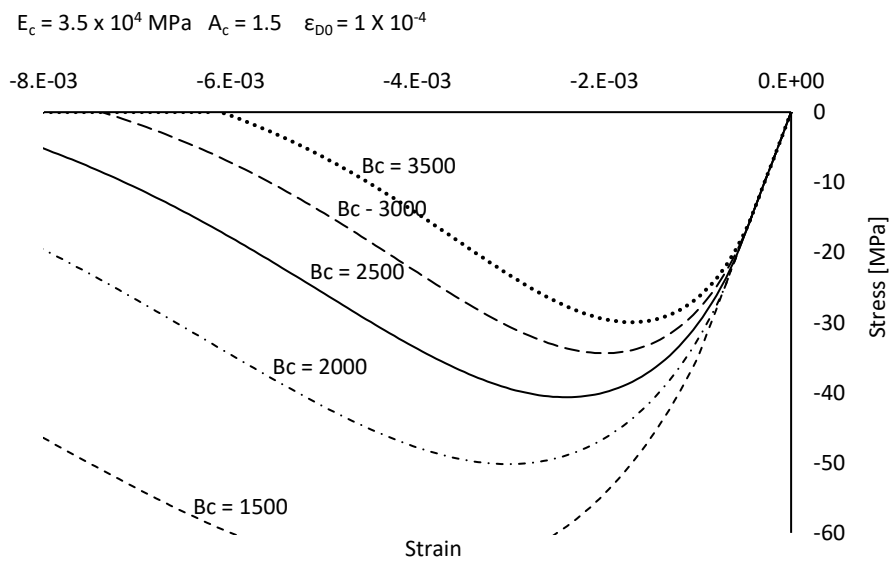


Figure 3.6. Influence of parameter B_c

As stated before, the scalar damage variable D is defined as a weighted sum of two damaging modes, one related to tension and the other related to compression. It is assumed that the damage in the material can only increase, not be recovered (i.e., closing of the cracks under reversed loading will not increase the stiffness of the concrete).

Results from the Mazars model were reported to underestimate the strength of panels when subjected to shear, as a result a coefficient β was added to reduce the effects of damage when the response is governed by shear, to address this limitation (Hamon, 2013). The value of the coefficient β is usually taken equal to 1.06. The modified expression for the weighted sum is shown in Eq. 3.10.

$$D = \alpha_t^\beta * D_t + \alpha_c^\beta * D_c; \quad 0 \leq D \leq 1 \quad (3.10)$$

To illustrate the uniaxial response of concrete according to the damage model by Mazars, Figure 3.7 shows the uniaxial stress-strain response in tension and compression of a concrete material with the following parameters: $E_c = 35,000$ MPa, $\varepsilon_{D0} = 0.0001$, $A_c = 1.57$, $B_c = 3,000$, $A_t = 0.97$, $B_t = 10,000$, $\nu = 0.18$, and $\beta = 1.06$. The loading path is as follows:

1. Compressive load is applied to the material until it reaches its maximum strength of 35 MPa at a strain of 0.002. The damage obtained at the peak stress of the material in this example is equal to 0.5.
2. The load is reversed and the strain in the material goes back to zero. The unloading path follows the initial stiffness reduced by the damage of 0.5.
3. Compressive load is again applied to the element. The reloading path is the same as the unloading path in the material, following the initial stiffness reduced by the damage of 0.5. Then, the material continues to be loaded until it reaches a strain of

0.004, double of that associated to the maximum compressive strength. The damage at this point is calculated to be equal to 0.83.

4. The load is reversed and the strain in the material goes to zero, following the unloading path of the initial stiffness reduced by the damage of 0.83.
5. Then, tensile load is applied to the element. As the material is damaged at this point with a value of 0.83, the tensile loading path follows the initial stiffness reduced by the damage of 0.83.
6. Tensile load is furthermore applied to the element, the damage in the material keeps increasing until it fails. The damage in the material is 1, and the element is completely cracked.

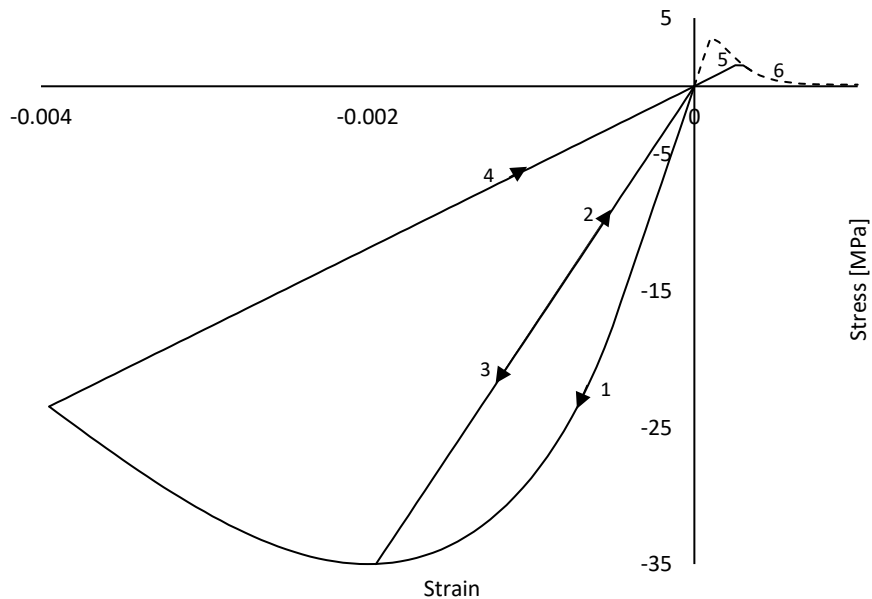


Figure 3.7. Uniaxial stress-strain response of Mazars model

The following phenomena are to be noted in the stress-strain response of the Mazars concrete model:

- The damage affects the stiffness of the concrete, modifying the unloading and reloading paths.
- The response in tension and compression are very asymmetrical, as is typical of a concrete material. This asymmetrical behaviour is generated by the A_t , B_t and A_c , B_c parameters in tension and compression respectively.
- The damage is non-recoverable in the concrete. Once the equivalent strain surpasses the damage threshold, the element will be irreversibly damaged. The damage will only increase as the loading cycles continue. In this example, the damage was equal to 0.5 even when the load was reversed, and it kept increasing after reloading the element until the value was 0.83.
- The material model does not account for permanent deformations. Damage only modifies the stiffness of the material, assuming complete recovery in the deformations of the element. This behaviour is a drawback of the material model, but helps in the simplicity of the element formulations.
- The damage created by either compressive or tensile strains will affect the behaviour of the element in both the tensile and compressive response.

3.3 Predictions and Comparison with FEA

Equations 3.1 through 3.10 were implemented in a spreadsheet and the Mazars concrete damage material model was used to predict the response of single and multiple plain concrete elements. The results are compared with two finite element analysis programs. One contains an implementation of the Modified Compression Field Theory, and the other implements a damage-based model. The two programs have been shown to accurately

represent the behaviour of plain and reinforced concrete shell elements under bidimensional loading (Lee and Kuchma, 2007; Luu et al. 2013; Mergos and Beyer, 2013; Lu et al. 2015).

3.3.1 Software Used for Comparison

The finite element analysis programs and frameworks were chosen to represent some of the theories available to describe the performance of reinforced concrete shell elements. They are known to represent accurately the behaviour of elements subjected to bidimensional static and dynamic loading. These programs are freely available under General Public License and are intended mainly for research purposes.

3.3.1.1 VecTor2 with Modified Compression Field Theory (MCFT)

VecTor2 is a program based on the Modified Compression Field Theory (Vecchio and Collins, 1986) and the Disturbed Stress Field Model (Vecchio, 2000), for nonlinear finite element analysis of RC membrane structures. The program has been developed at the University of Toronto since 1990, predicting the load-deformation response of a variety of RC structures exhibiting well-distributed cracking when subject to static, monotonic and cyclic loading.

3.3.1.2 OpenSees with PlaneStressUserMaterial (PSUMat)

OpenSees is a research-oriented framework for finite element analysis (Fenves, 2001). A key feature of the software is the interchangeability of components and the ability to

integrate existing libraries and new components into the framework without the need to change the existing code. A numerical model for concrete in two dimensions was developed and programmed in the OpenSees framework as Plane Stress User Material, termed as PSUMat (Lu et al. 2015). This material is a bidimensional, damage-based material model for use in shell elements, but the source code is proprietary and has not been released by the developers. It is included here as a reference.

3.3.2 Model Description and Results

The first two models were selected to resemble the behaviour of plain concrete under uniaxial loading. Single 200 x 200 mm elements, with 100 mm thickness were used in the analysis. All of the analyses are considered to be under the plane stress theory.

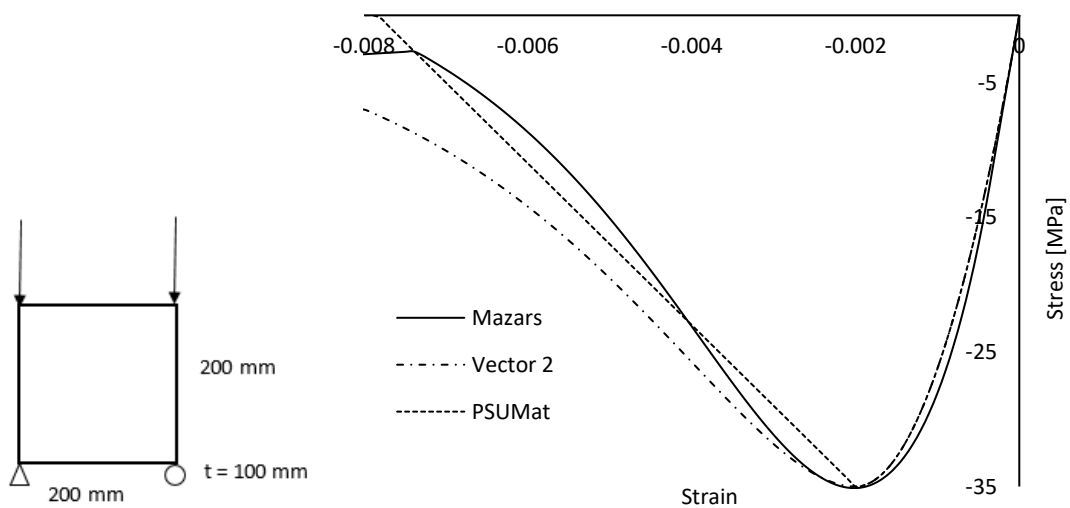


Figure 3.8. Stress-strain response of 1 plain concrete element subjected to pure compression

Figure 3.8 shows the stress-strain response of a single plain concrete element subjected to pure compression. The boundary conditions of the element allow it to distribute the

stresses in a single direction, resembling the traditional stress-strain curve for concrete in compression. All of the different theories describe the pre-peak behaviour of concrete as a curve, but only VecTor2 with MCFT and the Mazars model describe the post-peak behaviour as a curve. The drop in the strength resistance of concrete is given by the collapse of the cement-aggregate matrix and the appearance of micro-cracks in the orthogonal direction. Thus, a soft transition in the curve is expected in the post-peak behaviour, unlike the straight line observed with the Plane Stress User Material (PSUMat) in OpenSees.

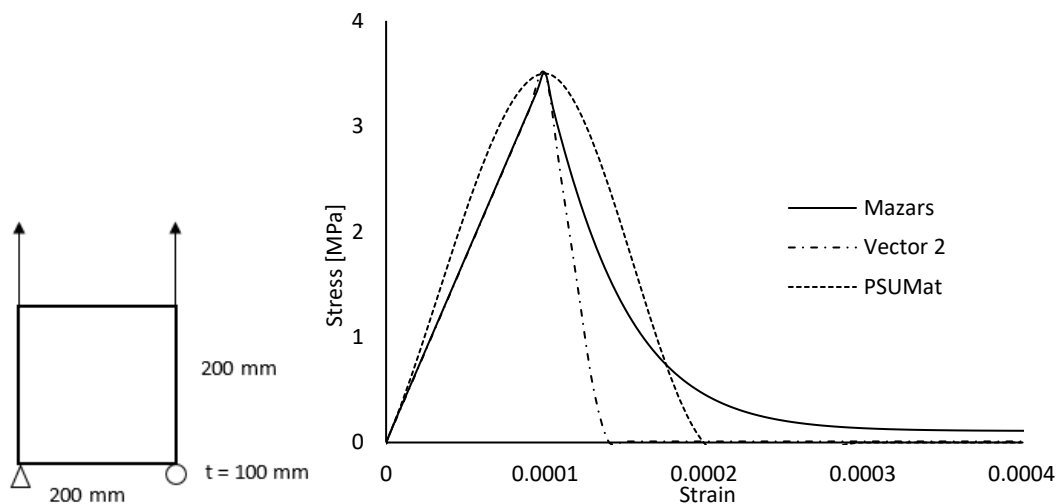


Figure 3.9. Stress-strain response of 1 plain concrete element subjected to pure tension

Figure 3.9 shows the stress-strain response of a single plain concrete element subjected to pure tension. The same boundary conditions are applied to the element to resemble the uniaxial tensile resistance of concrete. The behaviour of concrete under tension is known to be elastic before the ultimate tensile strength, with an abrupt loss of strength when the concrete cracks. This behaviour is accurately represented by both the Mazars model and

VecTor2 with MCFT. The soft transition given by the PSUMat in OpenSees is not expected when dealing with tensile stresses in unreinforced concrete.

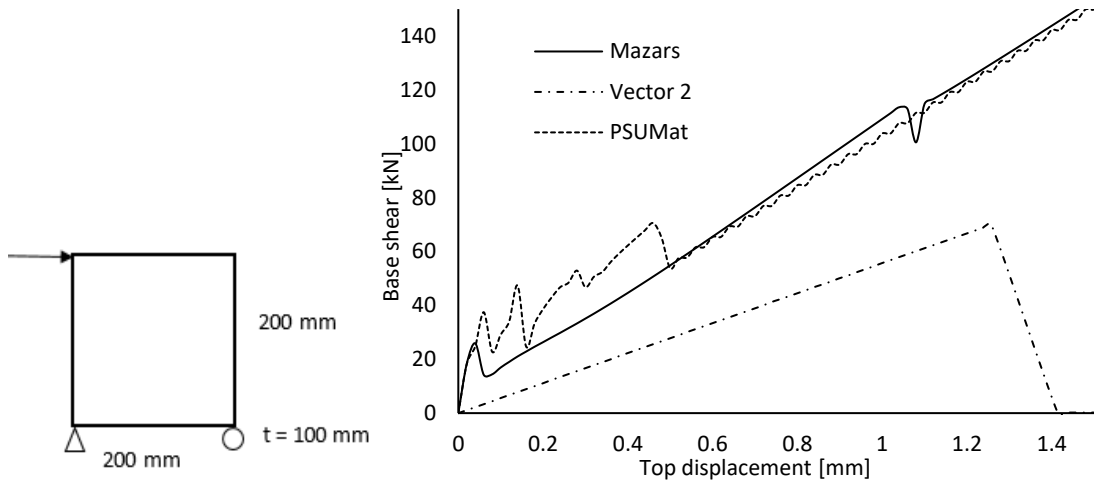


Figure 3.10. Force-displacement of 1 plain concrete element subjected to a lateral load

Figure 3.10 shows the force-displacement response of a single plain concrete element subjected to a lateral force, this is done to generate shear and normal stresses in the element. From this test, the two models that show the closest response are the damage based models (Mazars and PSUMat), they show a greater shear resistance than the one presented in VecTor2 with MCFT, this is given by the fact that the damage models account for post-crack shear resistance for the element, whereas in the MCFT formulation a steel reinforcement is needed to have this type of phenomenon.

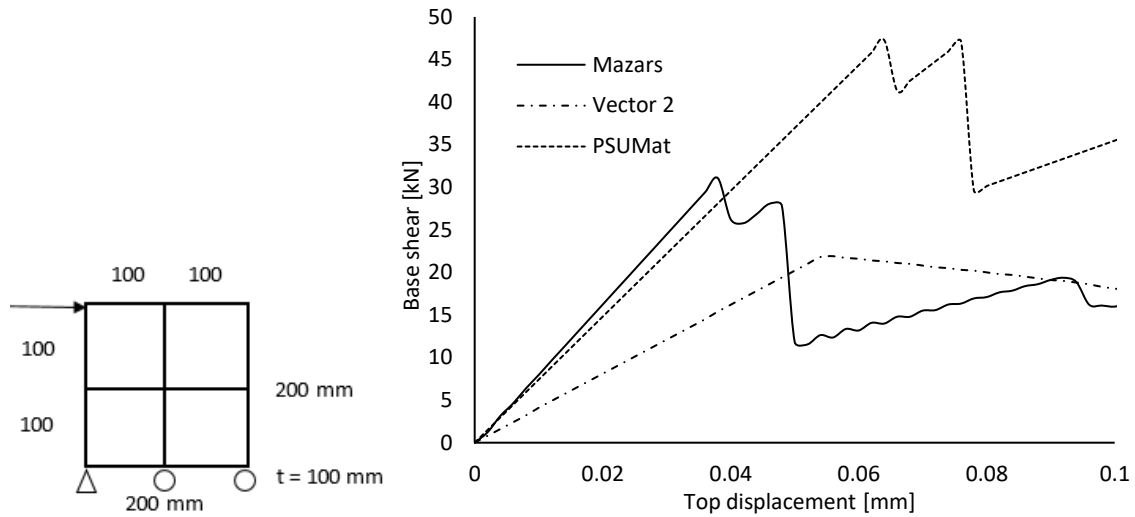


Figure 3.11. Force-displacement of 4 plain concrete elements subjected to a lateral load

Figure 3.11 shows the force-displacement response of a plain concrete shell with four square elements subjected to a lateral force in the top left corner element. All the elements will have a combination of normal and shear stresses. As expected the damage based models (Mazars and PSUMat) show a stronger resistance to shear forces, with failure occurring when the first crack appears, but continuing to have lateral resistance from the post-crack shear resistance of the element and the redistribution of the stresses within the structure itself.

3.4 Development of a Nonlinear 2D Material Model in the OpenSees Interface

The Mazars concrete damage model (Mazars, 1984) is implemented in the finite element framework OpenSees for 2D plane-stress elements. The coordinate system, equilibrium and compatibility equations used in the Mazars model are described in a finite element formulation, resulting in a material constitutive matrix of concrete based on the Mazars model. The material constitutive matrix is presented in its secant formulation.

3.4.1 OpenSees

The Open System for Earthquake Engineering Simulation (OpenSees) is a computational platform for structural performance simulation developed within the Network for Earthquake Engineering Simulation (NEES) project. The behaviour of structural and geotechnical systems can be simulated using a modular approach in OpenSees. These modules contain independently defined model configurations, numerical solutions, and output recorders. The flexibility of this modular implementation in OpenSees enables researchers to implement new components, such as material models, element types, and solution algorithms, as they are developed.

OpenSees uses the Tcl script language to write an input file which includes the structural model, the analysis type, and the required output recorders. The OpenSees source code is written in C++ language, using an object-oriented programming, which allows the creation of new classes or modules as parts of the framework.

3.4.1.1 Multi-layer Shell Element in OpenSees

The element selected to model plane structures under in- and out-of-plane loads in the OpenSees framework is the ShellMITC4 element, which is a four-node shell element based on the theory of mixed interpolation of tensorial components (MITC) (Dvorkin et al. 1995). The layered element simplifies the 3D nonlinear behaviour of the plane elements by discretizing them into several fully-bonded layers in the thickness direction. Different material properties and thicknesses can be assigned to each layer, as in Fig. 3.12. The stresses over a layer thickness are assumed to be consistent with those at the mid-surface of that layer (plane-stress theory). Therefore, if the plane component (for example, a shear

wall or a slab) is subdivided into a sufficient number of layers, the multi-layer shell element can reasonably simulate the actual stress distribution over the thickness of the shell. By using layered shell elements, the in-plane and the out-of-plane behaviour of a plane structure can be represented using biaxial element formulations.

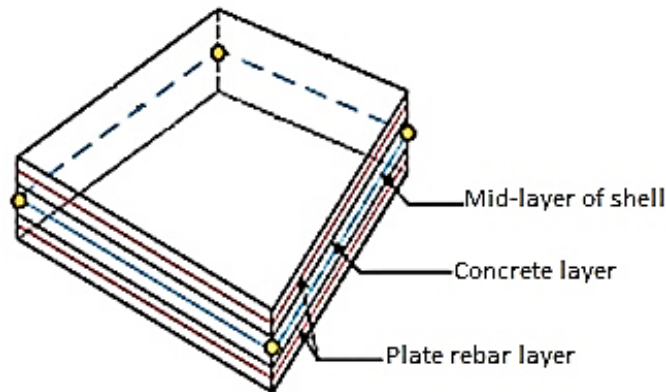


Figure 3.12. Multi-layer shell element

3.4.2 Coordinate System

Two Cartesian coordinates, x - y and 1 - 2 , are defined in the concrete elements, which are illustrated in Fig. 3.13. Coordinate x - y represents the local coordinates of the elements. The coordinate 1 - 2 defines the principal stress directions of the applied stresses, which have an angle of θ_1 with respect to the x - y coordinate.

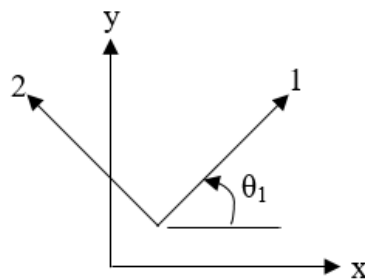


Figure 3.13. Coordinate systems for concrete elements

The stress and strain vectors in x-y coordinates and 1-2 coordinates are denoted as

$$\begin{Bmatrix} \sigma_x \\ \sigma_y \\ \tau_{xy} \end{Bmatrix}, \begin{Bmatrix} \varepsilon_x \\ \varepsilon_y \\ \frac{1}{2}\gamma_{xy} \end{Bmatrix}, \begin{Bmatrix} \sigma_1 \\ \sigma_2 \\ \tau_{12} \end{Bmatrix} \text{ and } \begin{Bmatrix} \varepsilon_1 \\ \varepsilon_2 \\ \frac{1}{2}\gamma_{12} \end{Bmatrix}, \text{ respectively. As the 1-2 coordinate represents}$$

the principal stress directions, τ_{12} is equal to zero in these vectors.

By using the transformation matrix $T(\theta_l)$, the stresses and strains can be transformed between the different coordinates.

$$T(\theta_1) = \begin{bmatrix} \cos^2(\theta_1) & \sin^2(\theta_1) & 2\sin(\theta_1)\cos(\theta_1) \\ \sin^2(\theta_1) & \cos^2(\theta_1) & -2\sin(\theta_1)\cos(\theta_1) \\ -\sin(\theta_1)\cos(\theta_1) & \sin(\theta_1)\cos(\theta_1) & \cos^2(\theta_1) - \sin^2(\theta_1) \end{bmatrix} \quad (3.11)$$

where θ_l is the angle between the x-y coordinates and the 1-2 coordinates, as seen in Fig. 3.13.

The stresses and strains transformed from the x-y coordinate to the 1-2 coordinate using the transformation matrix are expressed as follows:

$$\begin{Bmatrix} \sigma_1 \\ \sigma_2 \\ 0 \end{Bmatrix} = [T(\theta_1)] \begin{Bmatrix} \sigma_x \\ \sigma_y \\ \tau_{xy} \end{Bmatrix} \quad (3.12)$$

$$\begin{Bmatrix} \varepsilon_1 \\ \varepsilon_2 \\ 0 \end{Bmatrix} = [T(\theta_1)] \begin{Bmatrix} \varepsilon_x \\ \varepsilon_y \\ \frac{1}{2}\gamma_{xy} \end{Bmatrix} \quad (3.13)$$

3.4.3 Material Constitutive Matrix

A material constitutive matrix, also known as the material stiffness matrix, relates the state of stresses and strains for an element. It can be expressed in terms of secant or tangent

formulations. The secant material constitutive matrix relates the absolute values of strains and stresses of the element, and the tangent material constitutive matrix relates the increment of the stresses and strains of the element. Given that damage theories employ elastic theory for the material, a secant material constitutive matrix approach was selected.

The secant material constitutive matrix Γ for a plane stress element with an elastic isotropic material is given by:

$$\Gamma = \frac{E}{(1+\nu)} \begin{bmatrix} \frac{1}{1-\nu} & \frac{\nu}{1-\nu} & 0 \\ \frac{\nu}{1-\nu} & \frac{1}{1-\nu} & 0 \\ 0 & 0 & \frac{1}{2} \end{bmatrix} \quad (3.14)$$

Given the fact that the Mazars model is developed for the analysis of concrete in three dimensions, the analysis of the element needs to be done in three dimensions, adopting the axial strain in the out-of-plane direction assumed in plane stress theory. The use of the 3D properties of the concrete is useful for plane elements that are subjected to biaxial compression, where otherwise it would be impossible to obtain the equivalent strain as it is defined by tensile strains in the orthogonal directions of the applied stress.

In the plane stress assumption, the material can expand and contract freely in the third direction, which would be the thickness of the element. The corresponding value of the axial strain in the thickness direction, ε_z , can be obtained with

$$\varepsilon_z = -\frac{\nu}{E} * (\sigma_x + \sigma_y) \quad (3.15)$$

With this assumption, the principal strain ε_3 will always be the out-of-plane strain obtained using the plane stress theory, ε_z .

The initial material constitutive matrix Γ_c for concrete in three dimensions is given by.

$$\Gamma_c = \frac{E_c}{(1+\nu)(1-2\nu)} \begin{bmatrix} 1-\nu & \nu & \nu & & & \\ \nu & 1-\nu & \nu & & & \\ \nu & \nu & 1-\nu & & & \\ & & & \frac{1-2\nu}{2} & 0 & 0 \\ & & & 0 & \frac{1-2\nu}{2} & 0 \\ & & & 0 & 0 & \frac{1-2\nu}{2} \end{bmatrix} \quad (3.16)$$

while its corresponding inverted material constitutive matrix Γ_c^{-1} is given by.

$$\Gamma_c^{-1} = \begin{bmatrix} \frac{1}{E_c} & -\frac{\nu}{E_c} & -\frac{\nu}{E_c} & & & \\ -\frac{\nu}{E_c} & \frac{1}{E_c} & -\frac{\nu}{E_c} & & & \\ -\frac{\nu}{E_c} & -\frac{\nu}{E_c} & \frac{1}{E_c} & & & \\ & & & \frac{2(1+\nu)}{E_c} & 0 & 0 \\ & & & 0 & \frac{2(1+\nu)}{E_c} & 0 \\ & & & 0 & 0 & \frac{2(1+\nu)}{E_c} \end{bmatrix} \quad (3.17)$$

where E_c is the initial Young's modulus of the concrete, and ν is the Poisson's ratio.

The material constitutive matrix relates the concrete principal stresses σ_p and strains ε_p as given by

$$\{\sigma_p\} = (1 - D)[\Gamma_c]\{\varepsilon_p\}$$

where D is the damage in the material calculated from Mazars theory (Eqs. 3.1 – 3.10)

3.4.4 Analysis Procedure of Concrete Plane Stress Structures

After the damaged-material constitutive matrix Γ_{cD} is determined, the element stiffness matrix is evaluated using the basic finite element procedure dependent on the type of element used, and is expressed as:

$$[K] = \int [B]^T [\Gamma_c]_D [B] dV \quad (3.18)$$

where B is a matrix that depends on the element displacement functions.

There are several solution schemes to perform nonlinear analyses of reinforced concrete structures. One option is to use static integrators such as in displacement-controlled analysis, or dynamic integrators such as the Newmark method. There are also several possible solution algorithms such as the Modified Newton method, and the Krylov-Newton method. For the sake of simplicity, the flow chart for an iterative analysis solution, described in Fig. 3.14, performs a static analysis using load increment with the Newton-Raphson method.

In each iteration, the damaged material stiffness matrix $\Gamma_c D$ is determined using the Mazars material model described previously, and the element stiffness matrix K and the element resisting force increment vector ΔF are calculated. The damaged material constitutive matrix $\Gamma_c D$ and the element stiffness matrix are iteratively refined until convergence criterion is achieved.

The procedure for establishing the damaged material constitutive matrix using the Mazars model is shown in Fig. 3.14. It should be noted that this procedure does not require an iterative procedure to establish the damaged material constitutive matrix, making the Mazars model computationally efficient for finite element analysis. The source code developed in this research obtains the input strains of the element and calculates the corresponding stresses in the material, i.e. the procedure presented in the dotted square in Fig. 3.14.

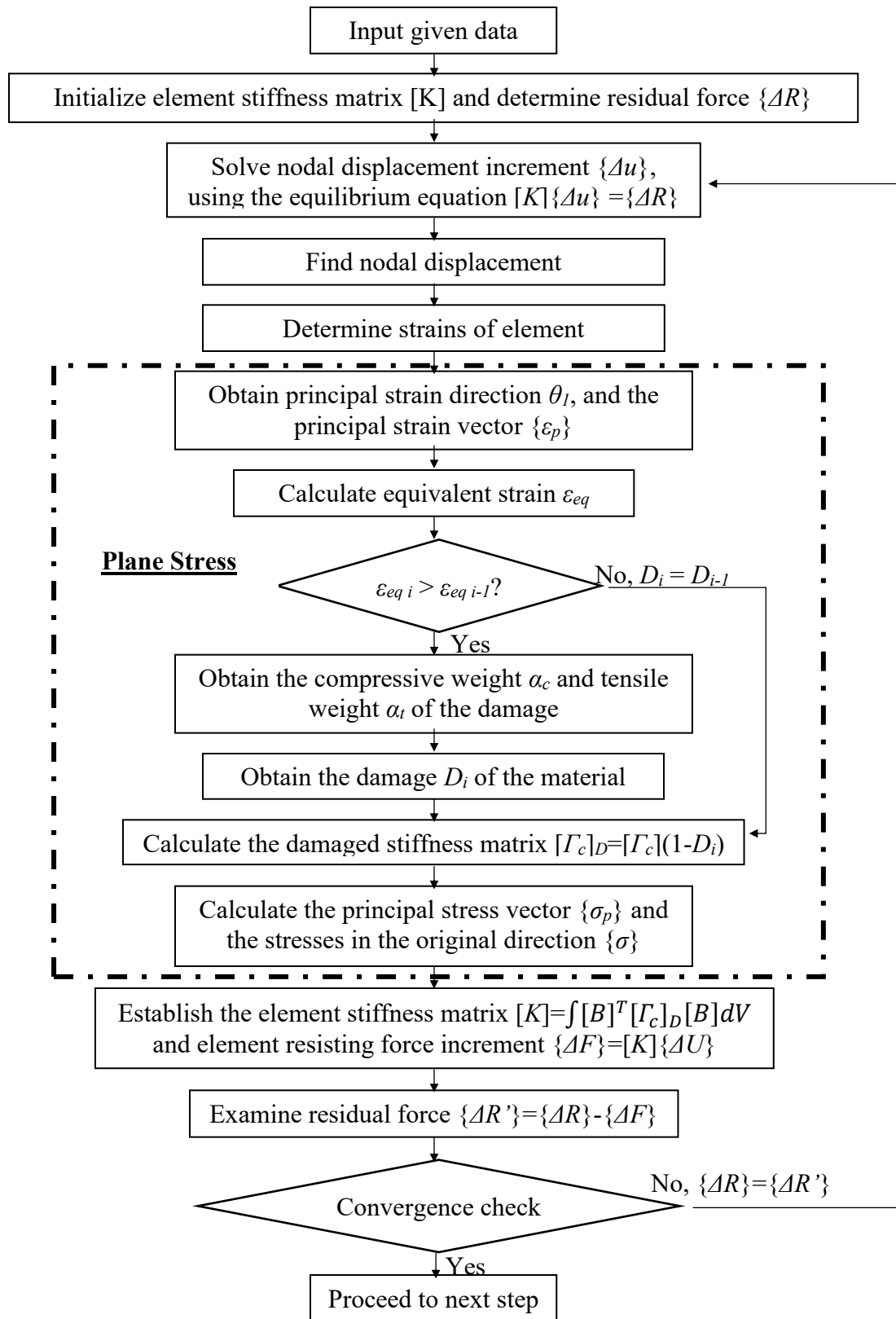


Figure 3.14. Nonlinear analysis algorithm

3.5 New ND Material Model in the OpenSees Framework

In order to perform analysis on reinforced concrete plane stress structures, a new material class is implemented into the OpenSees framework. The plane stress concrete material with the Mazars Damage model needs the following input parameters:

Box 1. Mazars Material Model

```
nDMaterial Mazars $matTag $Ec $epsD0 $Ac $Bc $At $Bt $nu
```

Where \$matTag is the unique material object integer tag, \$Ec is the initial Young's modulus of the concrete, \$epsD0 is the initial damage threshold, \$Ac and \$Bc are material parameters that define the compressive behaviour of the concrete, \$At and \$Bt are material parameters that define the tensile behaviour of the concrete, and \$nu is the Poisson's ratio.

3.5.1 Methodology. Adding a New Multi-Dimensional Material, nDMaterial

The modular and hierarchical nature of the OpenSees software, as seen in Fig. 3.15b), allows new material models to be added to the framework by keeping element and material implementations separate. A new material model can be used in an existing element without modifying the element implementation. Figure 3.15a shows the modules necessary for the OpenSees solution to create the executable file (OpenSees.exe). These modules have their own sub-classes.

The four essential steps needed to add a new multi-dimensional material model, nDMaterial, will be discussed next.

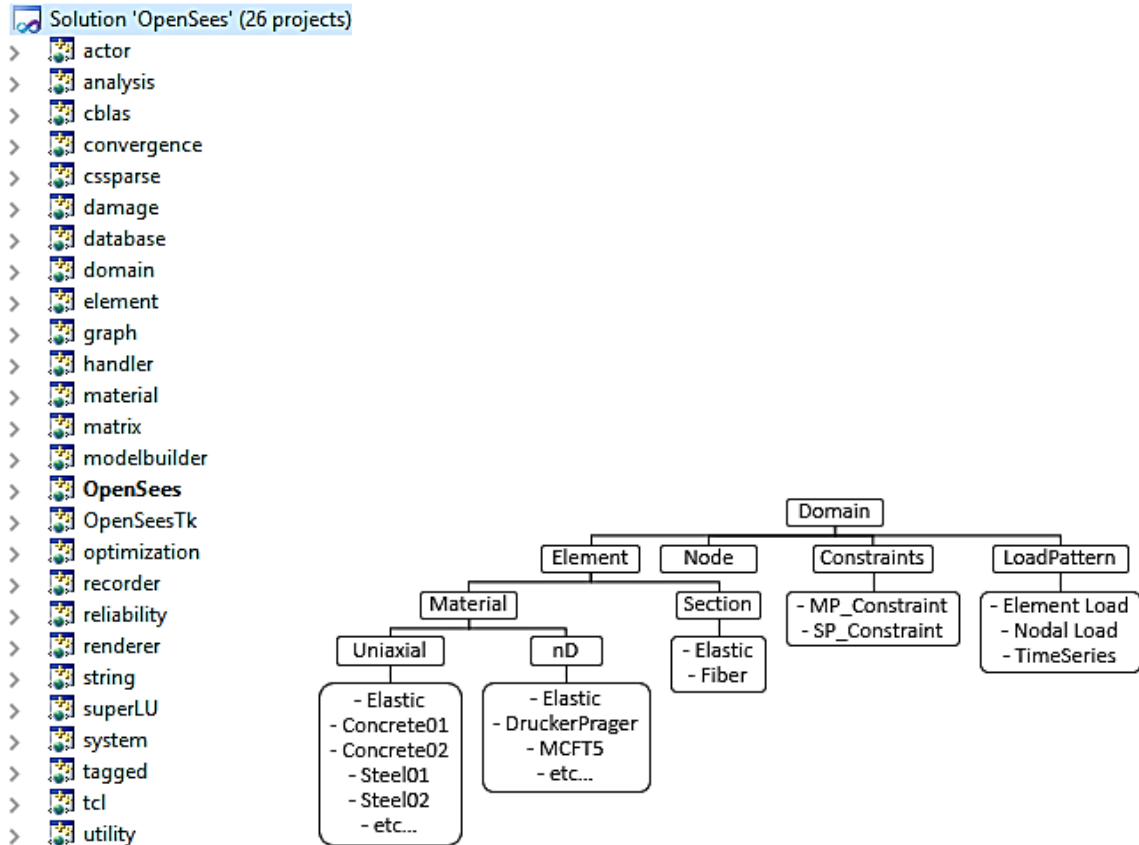


Figure 3.15. OpenSees Class Hierarchy. a) OpenSees application Solution, and b) Classes hierarchy

3.5.1.1 Constructor and Functions in the nDMaterial Class Interface

The nDMaterial class provides default implementations for the functions used to create a new subclass material model. The functions that are defined as virtual, i.e. the functions that contain '(void)' at the end of the function declaration, must be defined by the subclasses because the nDMaterial class does not provide a default implementation. The C++ source code for the Mazars model is shown in Appendix A. The inclusion of the C and C++ libraries necessary, and the declaration of the classes, functions and variables of the Mazars model is done in the Header File (Mazars.h). The implementation of these classes, functions and variables is done in the C++ File (Mazars.cpp). The declaration of

the constructors, functions and variables is presented next, and a brief description of some of the most important functions of the source code is given.

Box 2. Mazars Material Functions Declaration

```

class Mazars: public NDMaterial{
public :
    Mazars( ) ;
    Mazars(int tag, double _Ec, double _epsD0, double _Ac, double _Bc, double
_At, double _Bt, double _nu) ;

    virtual ~Mazars( ) ;
    void setInitials( ) ;

    NDMaterial *getCopy( ) ;
    NDMaterial *getCopy( const char *type ) ;

    int getOrder( ) const ;
    const char *getType( ) const ;

    int commitState( ) ;
    int revertToLastCommit( ) ;
    int revertToStart( ) ;

    int setTrialStrain( const Vector &strainFromElement ) ;

    const Vector& getStrain( ) ;
    const Vector& getStress( ) ;
    const Matrix& getTangent( ) ;
    const Matrix& getInitialTangent( ) ;

    void Print( OPS_Stream &s, int flag ) ;
    int sendSelf(int commitTag, Channel &theChannel);
    int recvSelf(int commitTag, Channel &theChannel, FEM_ObjectBroker
&theBroker);

private :
    Matrix iniTangent, tTangent, cTangent, iniSmallTangent, tangent;
    Matrix iniTangentInv, tTangentInv, cTangentInv;
    Vector tStrain, cStrain, strain, tStress, cStress, stress;
    double nu, Ec, epsD0, Ac, Bc, At, Bt, Beta;
    double fac, tDam, cDam, tepseq, cepseq;
} ;

```

Public functions in the declarations are accessible and modifiable by other classes in the OpenSees framework. These include the nDMaterial class virtual functions that need to be implemented in the new Mazars subclass, such as setTrialStrain(), getStrain(),

getStress(), and getTangent(). The function setTrialStrain(), takes the strain vector provided from the element to the material and defines the stress-strain relationship, this is where the element calculations of the Mazars model are executed (Fig. 3.14 and Eqs. 3.1-3.15); the functions getStrain(), getStress(), getTangent(), and getInitialTangent() return the current strain vector, stress vector, material tangent stiffness matrix, and initial tangent stiffness matrix, respectively, for the global coordinate system.

setInitials() is the function responsible to fill the vectors and matrices with the corresponding values. The initial stiffness matrix is filled with its values, and the vectors are filled with zeros that will be substituted with values from the element calculations.

The function commitState() is used to update the internal history variables at the converged solution path in the material. The function revertToLastCommit() is provided to return the history variables to the last committed state when convergence is not achieved in the current step. The function revertToStart() resets the history variables to their initial state.

The functions sendSelf() and recvSelf() communicate with other classes in the OpenSees framework. The function sendSelf() writes the material properties and the last committed history variable to a vector, and then sends it to the Channel object. The function recvSelf() receives data from the Channel object and imports the data of the Mazars object.

The functions getCopy() and getCopy(const char *type) are the functions in charge to create clones of the material, so it can be used in several elements within the same analysis.

OPS_Mazars(void) is the function responsible of the parsing of the material. This function makes sure that all the input values are provided and that they are valid values.

getOrder() and getType() are functions that communicate with the rest of the OpenSees modules, indicating the order of the strain vector needed, and the name of the material to execute.

The data in the private declaration of the Mazars class is only accessible from within the class itself. This is where the variables needed to perform the calculations in the material model are declared.

3.5.1.2 Class Tags

In order for the new Mazars material model to communicate with other classes in the OpenSees framework, a new internal class tag needs to be defined. This is done as follows:

Box 3. classTags

```
#define ND_TAG_Mazars 45
```

3.5.1.3 TclModelBuilderNDMaterialCommand

The new Mazars material model needs to be added to the OpenSees Tcl model builder to be used by the analysis models defined in the Tcl script input files. This command parses the material parameters in Tcl script input files and transfers them to the Mazars material constructor. The command is as follows:

Box 4. Tcl Model Builder

```
#include <Mazars.h>
.
.
.
void *
OPS_Mazars(void)
{
    NDMaterial *theMaterial = 0;
    int numArgs = OPS_GetNumRemainingInputArgs();
    if (numArgs != 8) {
        opserr << "Want: nDMaterial Mazars tag? Ec? epsD0? Ac? Bc? At? Bt? nu?" <<
endl;
        return 0;
    }
    int iData[1];
    double dData[7];
    int numData = 1;
    if (OPS_GetInt(&numData, iData) != 0) {
        opserr << "WARNING invalid integer tag: nDMaterial Mazars \n";
        return 0;
    }
    numData = 7;
    if (OPS_GetDouble(&numData, dData) != 0) {
        opserr << "WARNING invalid data: nDMaterial Mazars : " << iData[0] << "\n";
        return 0;
    }
    theMaterial = new Mazars(iData[0], dData[0], dData[1], dData[2], dData[3],
dData[4], dData[5], dData[6]);
    return theMaterial;
}
.
.
.

else if (strcmp(argv[1], "Mazars") == 0) {
    void *theMat = OPS_Mazars();
    if (theMat != 0)
        theMaterial = (NDMaterial *)theMat;
    else
        return TCL_ERROR;
}
```

3.5.1.4 FEM_ObjectBrokerAllClasses

The FEM_ObjectBrokerAllClasses returns an empty material object that can be populated with the data from the function recvSelf(). The nDMaterial model is modified to allow

parallel processing and database programming to the new Mazars material object. The FEM_ObjectBroker file needs to be modified, including the following:

Box 5. FEM_ObjectBrokerAllClasses

```
#include <Mazars.h>

.
.
.

NDMaterial*
FEM_ObjectBrokerAllClasses::getNewNDMaterial(int classTag)
{
    switch(classTag) {

case ND_TAG_Mazars:
        return new Mazars();
    }
}
```

3.6 Summary

The description of the material formulations from the Mazars concrete damage model are given, and parametric analyses for the influence of its variables are shown. The Mazars model is adapted for the use in biaxial elements in finite element analysis, using plane stress theory. Then, the model is implemented in the open-source, FEA framework OpenSees for the use in multilayer-shell elements. By doing so, the material model can be used for the modelling of 3D RC structures that contain plane elements such as shear walls, slabs or deep beams.

CHAPTER 4 – VERIFICATION

In this chapter, the Mazars Concrete Damage material implemented into the OpenSees computing platform is verified with experimental data.

4.1 Introduction

A new concrete material model was implemented in OpenSEES for use in 2D damage- based finite element analysis. The proposed material model is based on damage mechanics and is capable of modeling the biaxial behaviour of concrete under static and dynamic loadings. Three types of reinforced concrete structures are modelled using the OpenSees computing platform with the new Mazars concrete damage material and compared with test results. The first is a simply supported beam under monotonic load built and tested at the University of Alberta in 2013, the second is a cantilevered shear wall under cyclic loading tested by Hiotakis (2004), and the third is a full-scale, four-story reinforced concrete building with shear walls tested under biaxial seismic excitation at the E-Defense shake table facilities in Japan (Nagae et al. 2011a; 2011b; 2012).

4.2 Analysis of a RC Beam Under Monotonical Loading

A reinforced concrete beam was designed and tested as part of the Civ E 672 course, “Behaviour and Design of Reinforced Concrete Elements” at the University of Alberta in December 2013. The beam was simply supported and was subjected to four-point bending. The beam had a rectangular cross-section (Fig. 4.1). The section dimensions were

150 x 300 mm. The longitudinal reinforcement consisted of two 15M (16 mm) bars at the bottom of the beam, and two 10M (11.3 mm) bars at the top of the beam. Transverse reinforcement consisted 10M (11.3 mm) stirrups spaced at 220 mm on both ends of the beam. The beam supports were located at 2400 mm from each other, and the specimen was loaded with two point loads at 400 mm each from the beam centre line. The compressive strength of the concrete at the time of the test was 37.2 MPa, and the associated strain at peak stress was measured as 0.004. The yield stress of the reinforcing steel was measured as 475 MPa and the modulus of elasticity was 183,333 MPa. The strain- hardening modulus was calculated as 2,872 MPa, and the strain associated to onset of strain-hardening was 0.01. The beam was tested under quasi-static, monotonic load until failure. The failure mode consisted of buckling of the compressive reinforcement (top bars at the middle of the beam) and crushing of the concrete in compression (top of the beam, middle section).

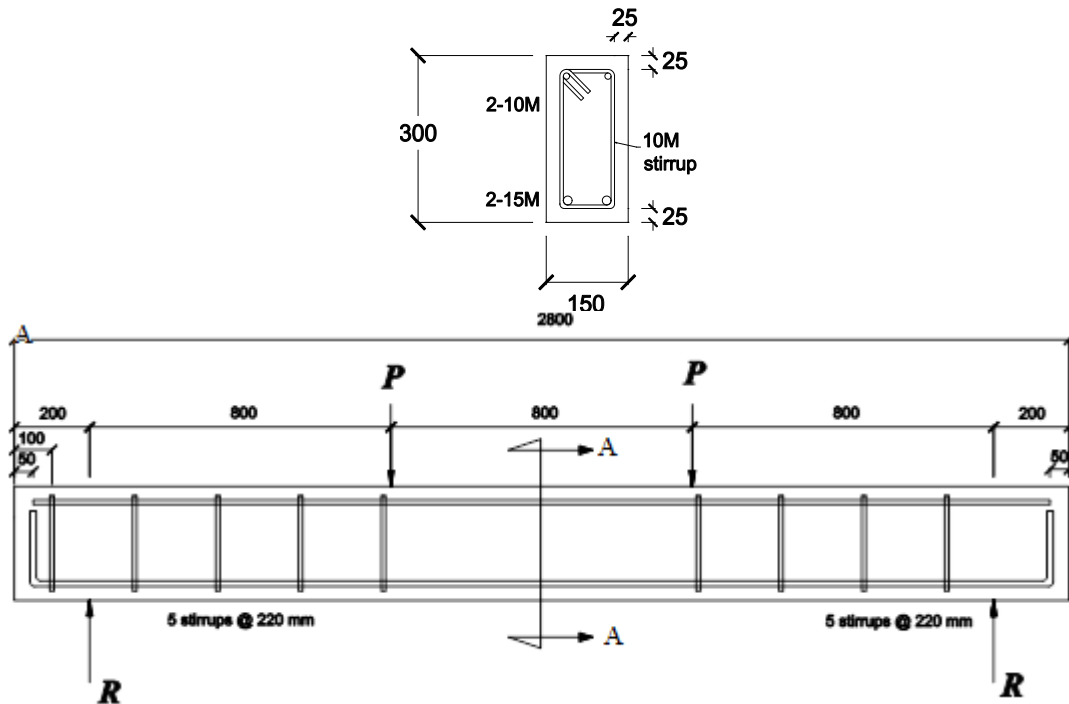


Figure 4.1. Beam geometric details. Dimensions in mm.

4.2.1 FEA Model and Analysis Method

The beam model was built in OpenSEES using 312 four-node multilayer-shell elements for the concrete (Fig. 4.2). Each element consisted of three layers with a thickness of 50 mm. For the steel reinforcement 140 truss elements were used. The adopted mesh was able to accommodate the steel reinforcement in their actual positions within the beam. The concrete was modelled using the new Mazars material. The parameters used to model the concrete were $E_c = 18602.98$ MPa, $\varepsilon_{D0} = 0.0002$, $A_c = 1.33$, $B_c = 1260.0$, $A_t = 0.97$, $B_t = 10,000.0$ and $\nu = 0.18$. The steel reinforcement was modelled using the Giuffre- Menegotto-Pinto steel model with isotropic strain hardening (Menegotto, 1978). Boundary conditions were set in nodes 5 and 49, they were restricted in the y-direction, while the middle of the beam was supported in the x-direction to allow for symmetry. The load was applied in two steps. First, the gravitational load was applied at all the top nodes of the beam and kept constant. Then, a displacement-controlled analysis was conducted by applying a downward displacement at nodes 337 and 353. The analysis was performed using the Krylov-Newton algorithm with current tangent for the iterations, given that is less computationally expensive in static and quasi-static analyses (Scott and Fenves, 2003). The nodal displacement and corresponding vertical forces were recorded at each converged displacement step.

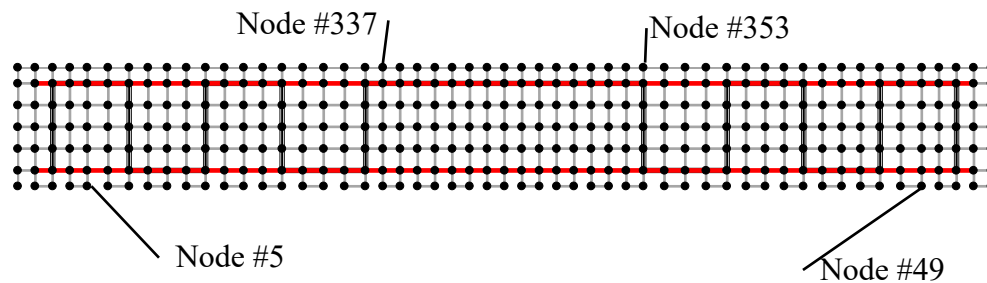


Figure 4.2. FEA model of RC beam

4.2.2 Comparison of Predictions and Experimental Results

The experimental and calculated load-deflection responses of the beam are shown in Fig. 4.3. The comparison of the load-deflection responses shows satisfactory agreement between the experiment and the analysis. However, the cracking moment of the beam was overestimated by the finite element model and yielding moment presented itself at a smaller strain in the test than the model. This is given by the overestimation of the tensile capacity of the concrete. The strain (ϵ_{θ}) at the maximum strength of the concrete measured in the tests was double of a regular concrete (0.004 vs. 0.002). To account for this increase in the strain, the strain at which the damage starts (ϵ_{D0}) in the Mazars' model needed to be increased accordingly. By having a single variable (ϵ_{D0}) representing where the damage starts in both tension and compression, the tensile response was affected as well, giving the material a higher tensile strength.

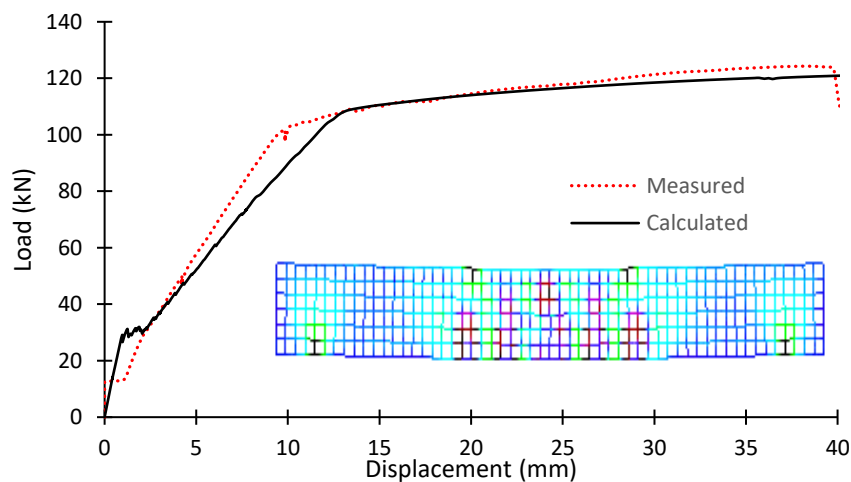


Figure 4.3. Analysis results of RC beam

The failure mode in both the test and the finite element model was given by the crushing of the concrete in compression. Buckling cannot be simulated by the steel material used in

the model, but despite this limitation the model had a satisfactory performance in predicting the failure displacement and load. This is explained because the occurrence of buckling and the onset of concrete crushing occurred simultaneously in the experiment.

4.3 Analysis of a RC Shear Wall Under Cyclic Loading

The experimental results obtained from the cantilevered, reinforced concrete wall tested by Hiotakis (2004) were used to validate the model performance under reversed, cyclic load. The wall specimen consisted of a cantilevered, 1.8 x 1.5 x 0.1 m shear wall specimen, a heavily reinforced foundation block, and a cap beam at the top for distribution of the applied load, as seen in Fig. 4.4. The wall was fixed to the laboratory strong floor through posttensioned rods to achieve a rigid connection. The wall was subjected to cyclic lateral loading, of increasing magnitude, applied at the cap beam through hydraulic actuators. The vertical reinforcement of the shear wall was composed of six pairs of 10M (11.3 mm) bars uniformly distributed along the wall and spaced at 280 mm, which corresponded to a steel reinforcement ratio (ρ_s) of 0.8%. The horizontal reinforcement of the shear wall consisted of five pairs of 10M (11.3 mm) bars uniformly distributed and spaced at 400 mm, which corresponded to a steel reinforcement ratio (ρ_s) of 0.5%. Closed stirrups consisting of 10M (11.3 mm) bars spaced at 80 mm along the height of the wall were anchored around the two extreme vertical reinforcement pairs as boundary reinforcement, for a reinforcement ratio (ρ_s) of 3.0%. The concrete compressive cylinder strength at the time of test was 36.2 MPa, and the yield stress of the reinforcing steel bars was 425 MPa.

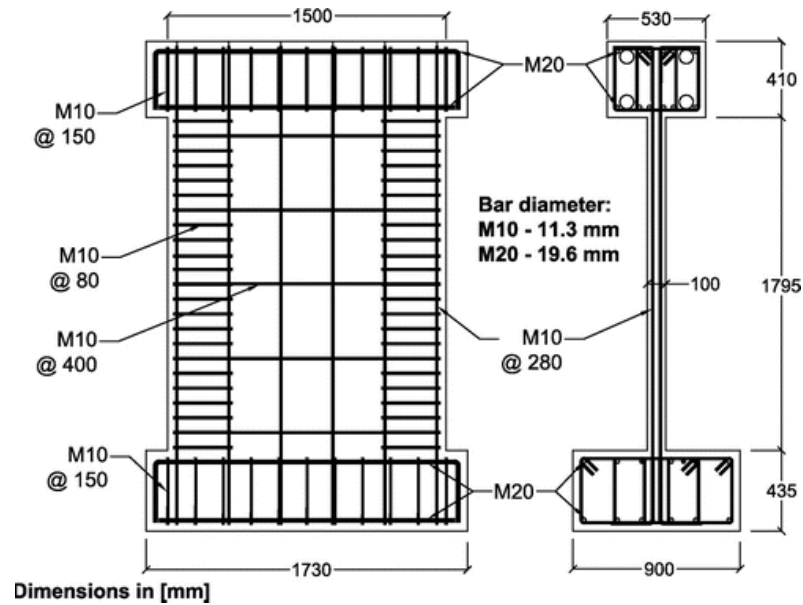


Figure 4.4. Shear wall geometric details (Hiotakis, 2004)

4.3.1 FEA Model and Analysis Method

A RC shear wall model for finite element analysis, using the new Mazars concrete damage material developed in the OpenSees framework, was created. The shear wall model was built using 270 four-node rectangular, multilayered shell elements, as seen in Fig. 4.5. The mesh was divided into two regions, the core and the boundaries, as indicated by the different shading. It was assumed that the cap-beams are far stiffer than the shear wall, so to keep the simplicity in the model, the bottom and top slab were not modelled and were instead considered by binding the horizontal degree of freedom of all the nodes in the top of the wall, and by fixing all the nodes at the base of the shear wall. A cyclic displacement history was applied to the centre top node of the wall in the horizontal direction, and the horizontal forces were recorded. The size of the elements at the wall core and boundaries are 100 x 100 mm.

To model the steel rebars and stirrups, the reinforcement ratios at the wall boundaries and core are assigned as uniformly-distributed reinforcement within the shell elements. This procedure allows for a more computationally efficient solution compared to modeling the reinforcement as truss elements, helping the model to reach convergence in each step when complex loading configurations are presented. The failure criterion for steel reinforcement was fracture in tension.

The layers for the shell elements were divided in concrete layers and steel reinforcement layers. The thickness of the concrete in the shear wall (t_c) was divided into several layers with similar thicknesses. The thickness of the reinforcing steel was calculated using Eq. 4.1, obtaining a relative steel thickness (t_s) for each of the steel layers.

$$\rho_s = \frac{A_s}{A_c} = \frac{t_s}{t_c} \quad (4.1)$$

The multilayer-shell elements at the wall boundaries consisted of 12 layers. The two outer-most layers were the unconfined concrete cover with a thickness of 12.5 mm each, two layers consisting of the stirrups with a thickness (t_s) of 0.8889 mm each, two layers consisting of the horizontal reinforcement with a thickness of 0.2778 mm each, two layers consisting the vertical reinforcement with a thickness of 0.4 mm each, and four layers consisting of the confined concrete with a thickness of 17.96665 mm each.

The multilayer-shell elements at the wall core consisted of 8 layers. The two outer-most layers were the unconfined concrete cover with a thickness of 12.5 mm each, two layers consisting of the horizontal reinforcement with a thickness of 0.2778 mm each, two layers consisting the vertical reinforcement with a thickness of 0.4 mm each, and two layers consisting of the unconfined concrete with a thickness of 36.8222 mm each.

The concrete at the boundaries of the wall was modeled as confined due to the presence of additional stirrups, as seen in Fig. 4.4, and unconfined concrete was used for the wall core. The response of the concrete was modeled with the new Mazars concrete damage material, and concrete failure was considered to occur when the crushing strength in compression was reached. The Mazars model was developed to represent the behaviour of normal-strength unconfined concrete, but by adjusting the material parameters (ϵ_{D0} , A_c , B_c , A_t , B_t), confinement properties as per Mander's model were simulated in the concrete material.

The parameters used to model the unconfined concrete were $E_c = 30,000$ MPa, $\epsilon_{D0} = 0.00008$, $A_c = 1.55$, $B_c = 2,700$, $A_t = 0.97$, $B_t = 7,000.0$ and $\nu = 0.18$. And the parameters used to model the confined concrete were $E_c = 30,000$ MPa, $\epsilon_{D0} = 0.00008$, $A_c = 0.5$, $B_c = 1,200$, $A_t = 0.97$, $B_t = 7,000.0$ and $\nu = 0.18$.

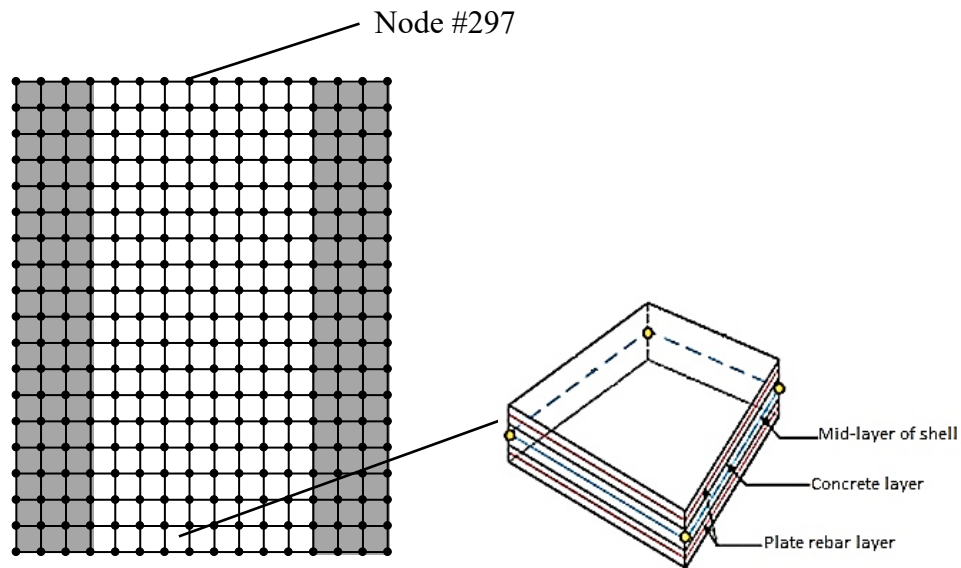


Figure 4.5. FEA model of RC shear wall

The load pattern in the finite element model is defined per the test conditions. The cyclic load was applied as a horizontal nodal displacement at node 297 (Fig. 4.5), which varied

according to the displacement control scheme. The file includes the material model assignment for each element, analysis method, and nonlinear solution algorithm. The Krylov-Newton algorithm with current tangent for the iterations was selected for the analysis. The nodal displacement and corresponding horizontal forces were recorded at each converged displacement step, and stress and strain of the elements were monitored.

4.3.2 Comparison of Predictions and Experimental Results

The calculated vs. measured global base shear-top displacement response of the shear wall is presented in Fig. 4.6.

It is seen that the maximum strength and displacement calculated at each cycle with the model has a reasonable correspondence with the measured results. However, the predictions for the hysteretic behaviour do not capture well the energy dissipation capacity (as given by the area within the hysteretic loops), residual displacement, and pinching effects seen in the experimental results. The difference in the analytical and experimental results is mainly in the unloading and reloading cycles of the specimen. The test reflects the common behaviour of concrete to develop plastic (residual) strains when damaged after each cycle. However, Mazars concrete damage model is not capable of reproducing this behaviour, the damage is only reflected in the stiffness of the material. The unloading and reloading paths after each cycle will always return to the origin of the stress-strain relationship in the Mazars model. So, the only plastic deformations observed in the shear wall calculated response, are generated from the residual strains in the steel reinforcement. A concrete damage model that separates the concrete curve in its 'elastic' and 'plastic' parts, could represent the residual strains that affect concrete.

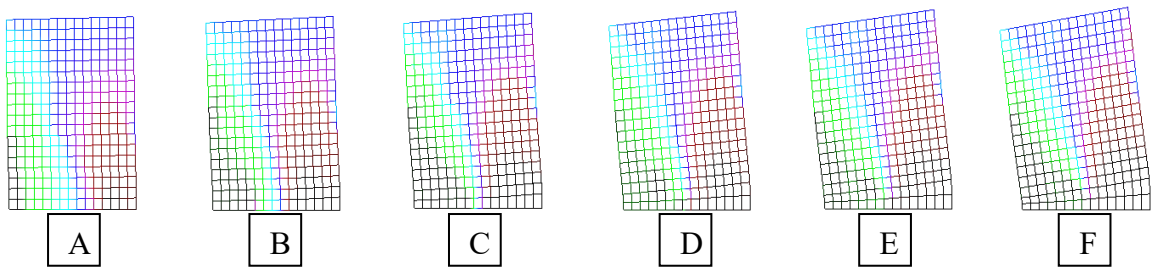
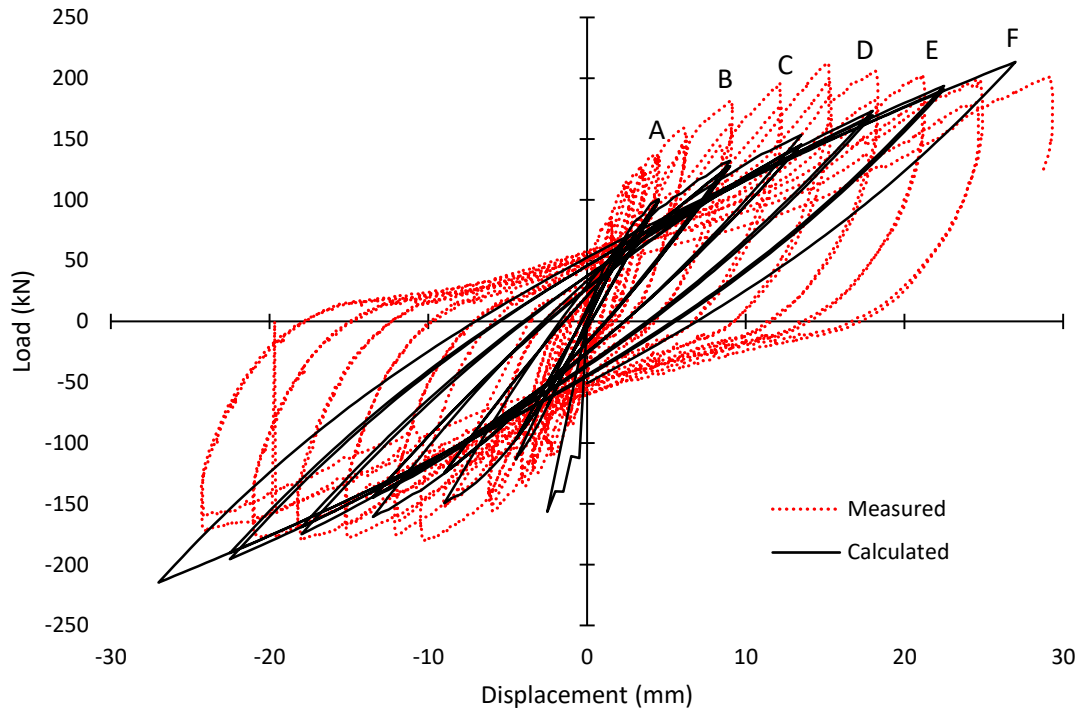


Figure 4.6. Cyclic analysis results of RC shear wall

4.4 Analysis of a Full-Scale Four-Story RC Building Under Seismic Loading

A full-scale building structure was tested by Nagae et al. (2015) using the E-Defense shaking table facility (Japan) in 2010. The structure was a four-story reinforced concrete building designed according to the Japanese seismic design code (AIJ, 1999 and 2010). The objective of the test was to assess the performance in service, design, and maximum considered earthquake shaking of full-scale structures designed under the current design codes for seismic regions.

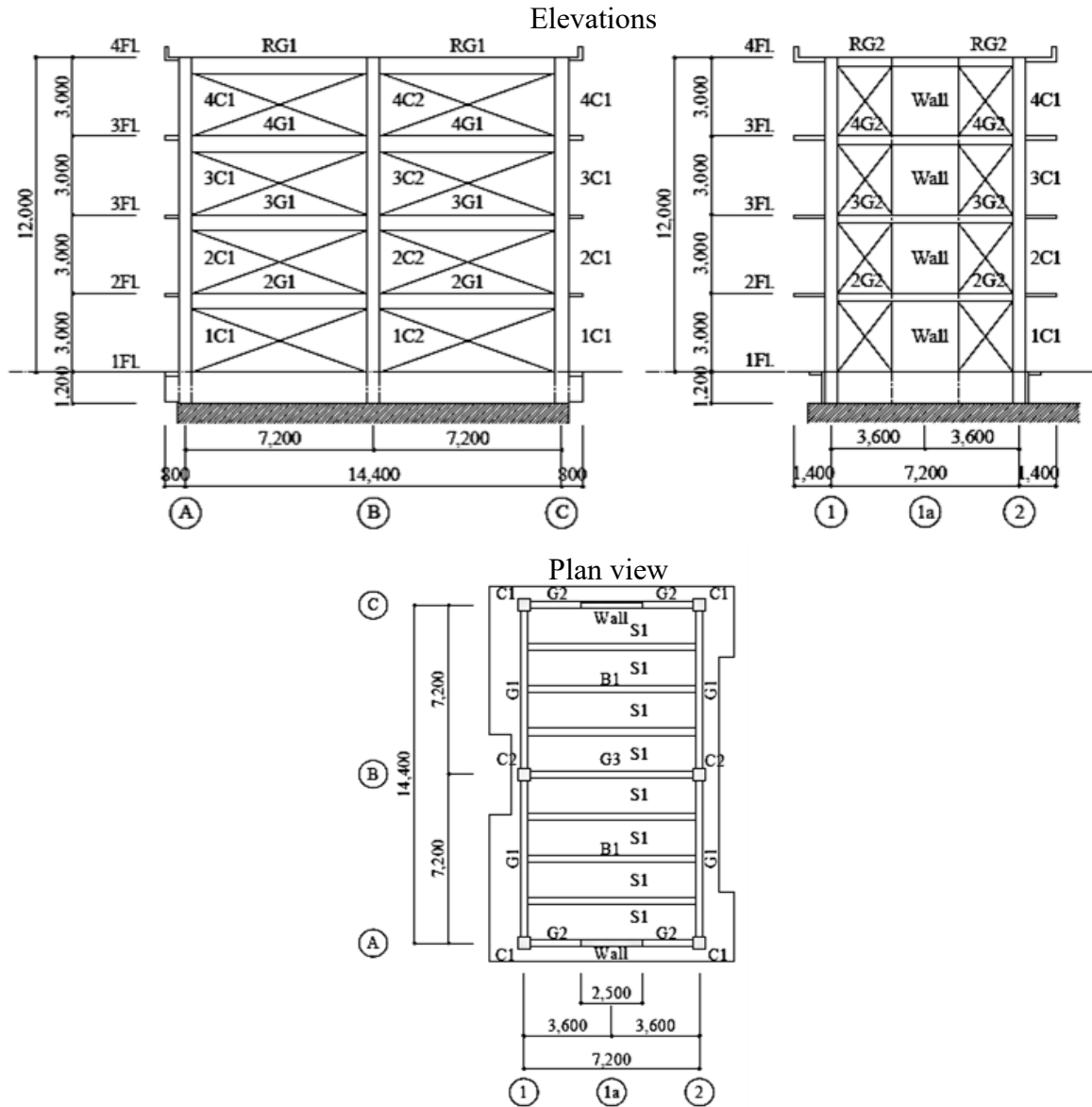


Figure 4.7. RC building geometric details (Nagae et al. 2011b)

Figure 4.7 shows the plan and framing elevations of the structure. The height of each story is 3 m. Lateral support in the longitudinal (L) direction was provided by means of a moment frame system of two spans of 7.2 m each, and in the transverse (T) direction a pair of multi-story RC shear walls were incorporated in the exterior frames of one span of 7.2 m. The foundations were fixed on the shaking table to transmit the full motion to the structure. The column sections of the structure were 500 x 500 mm. In the moment frame

of the L-direction, the beam depth was 600 mm, and in the T-direction, the wall section was 250 x 2500 mm. Walls were coupled to the corner columns by beams with a depth of 300 mm. The thickness of the top slab was 130 mm and the foundation beam had a depth of 1200 mm.

Table 4.1 shows the complete list of the cross-section dimensions and reinforcement for the RC elements of the structure. The building was designed following the Japanese Building Standard for RC building. The concrete specified design strength was 27 MPa, the longitudinal reinforcement had a nominal yield strength of 345 MPa, and the shear reinforcement had a nominal yield strength of 295 MPa. Table 4.2 shows the actual material properties at the time of the test. The diameters of the longitudinal reinforcement of the beams and columns were 22 mm and 19 mm, while the reinforcement at the walls were 19 mm and 13 mm, and the diameter of the shear reinforcement was 10 mm.

The weight of the structure was estimated considering the structural members, the measuring equipment, and safety steel frames. The weights of the floors of the building were 867 kN for the second floor, 872 kN for the third floor, 867 kN for the fourth floor, and 934 kN for the roof, for a total weight of the structure estimated at 5877 kN.

List of Column			
		C1	C2
4FL 3FL	Section		
	B x D	500 x 500	500 x 500
	Rebar	8-D22	10-D22
	Hoop	2,2-D10@100	2,2-D10@100
	Joint	2,2-D10@140	2,2-D10@140
2FL	Section		
	B x D	500 x 500	500 x 500
	Rebar	8-D22	10-D22
	Hoop	2,3-D10@100	2,4-D10@100
	Joint	2,2-D10@140	2,2-D10@140
1FL	Top Section		
	B x D	500 x 500	
	Rebar	8-D22	
	Hoop	2,3-D10@100	
	Joint	2,2-D10@140	
	Bottom Section		
	B x D	500 x 500	
Rebar	10-D22		
Hoop	3,4-D10@100	3,4-D10@100	
Joint	2,2-D10@140	2,2-D10@140	

List of Wall				
	Wall			
4FL 3FL 2FL	Section			
	B x D	2,500 x 250		
	Rebar	2 x 6-D19	Vertical	D13@300 (W)
	Hoop	2,2-D10@100	Horizontal	(A) D10@125 (W) (C) D10@200 (W)
	Joint	2,2-D10@150		
1FL	Section			
	B x D	2,500 x 250		
	Rebar	2 x 6-D19	Vertical	D13@300 (W)
	Hoop	(A) 2,3-D10@80 (C) 2,3-D10@100	Horizontal	(A) D10@125 (W) (C) D10@200 (W)
	Joint	2,2-D10@150		
	List of Slab Depth: 130mm			
	S1	Top	Shorter direction	Longer direction
Bottom		D10@200	D10@250	
CS1	Top	D10,D13@200	D10@250	
	Bottom	D10@200	D10@250	
CS2	Top	D10@200	D10@250	
	Bottom	D10@200	D10@250	
CS3	Top	D10,D13@200	D10,D13@200	
	Bottom	D10@200	D10@200	

List of Girder					
	G1				
	Location	End	Center	End	
RF1 4FL	Section				
	B x D	300 x 600			
	Top	4-D22	3-D22	4-D22	
	Bottom	3-D22	3-D22	3-D22	
	Web	4-D10			
	Stirrup	2-D10@200			
	3FL	Section			
B x D		300 x 600			
Top		5-D22	3-D22	5-D22	
Bottom		3-D22	3-D22	3-D22	
Web		4-D10			
Stirrup		2-D10@200			
2FL		Section			
	B x D	300 x 600			
	Top	6-D22	3-D22	6-D22	
	Bottom	3-D22	3-D22	3-D22	
	Web	4-D10			
	Stirrup	2-D10@200			

List of Girder				
	G2			
	Location	End	Center	
RF1	Section			
	B x D	300 x 300		
	Top	3-D19	3-D19	
	Bottom	2-D19	3-D19	
	Web	-		
	Stirrup	2-D10@100(KSS785)		
	4FL 3FL 2FL	Section		
B x D		300 x 300		
Top		3-D19	4-D19	
Bottom		3-D19	3-D19	
Web		-		
Stirrup		2-D10@100(KSS785)		

List of Girder				
	G3			
	Location	End	Center	
4FL 3FL 2FL	Section			
	B x D	300 x 400		
	Top	5-D19	3-D19	
	Bottom	3-D19	4-D19	
	Web	2-D10		
	Stirrup	2-D10@200		
	1FL	Section		
B x D		300 x 400		
Top		4-D19	3-D19	
Bottom		3-D19	4-D19	
Web		2-D10		
Stirrup		2-D10@200		

List of beam				
	B1			
	Location	End	Center	
All	Section			
	B x D	300 x 400		
	Top	3-D19	3-D19	
	Bottom	4-D19	7-D19	
	Web	2-D10		
	Stirrup	2-D10@200		

Table 4.1. List of reinforcing steel (Nagae et al. 2011b)

Steel					Concrete			
	Grade	A_{normal} (mm ²)	σ_y (N/mm ²)	σ_t (N/mm ²)		F_c (N/mm ²)	σ_B (N/mm ²)	Age (Days)
D22	SD345	387	370	555	1st - 2nd floor	27	39.6	91
D19	SD345	287	380	563	2nd - 3rd floor	27	39.2	79
D13	SD295	127	372	522	3rd - 4th floor	27	30.2	65
D10	SD295	71	388	513	4th - roof floor	27	41.0	53
D10*	SD295	71	448	545				
D10*	KSS785	71	952	1055				

Table 4.2. RC building actual material properties (Nagae et al. 2011b)

The Kobe records for the 1995 Hyogoken-Nanbu earthquake were the input ground motions used in the test. The accelerograms in the North-South, East-West, and Up-Down directions were provided as input motions for the longitudinal direction, transverse direction, and vertical direction respectively. The acceleration records for the seismic motions are presented in Fig. 4.8. The intensity of the motions was gradually increased during the test to observe the damage process in the structure. The intensity increments for the Kobe record were 25%, 50%, and 100% of the recorded motions for the earthquake.

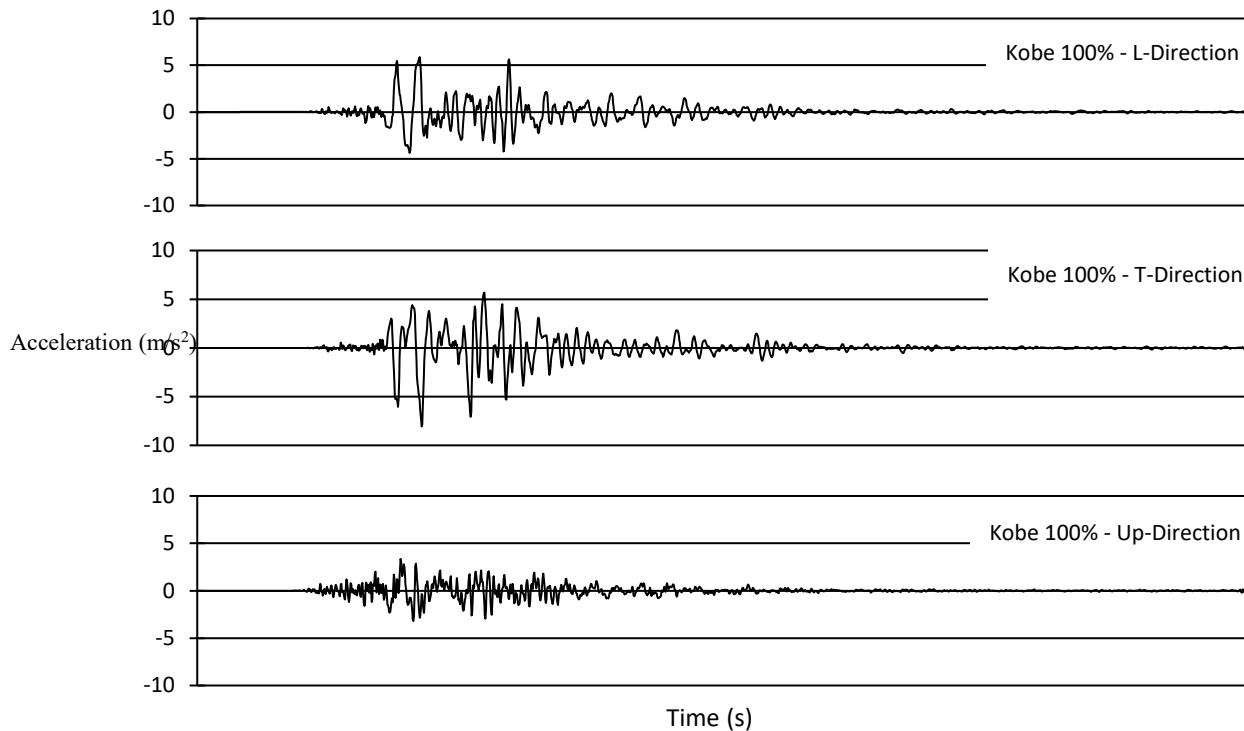


Figure 4.8. Input ground motions

4.4.1 FEA Model and Analysis Method

A model was developed in the OpenSees framework with the new Mazars concrete damage material that described the behaviour of the full-scale RC building. Due to the complexity of the structure, different types of elements and materials in the OpenSees framework were used to create the model. Figure 4.9 shows the finite element model in the OpenSees framework.

Columns and beams were created using linear uniaxial elements with cross-sections composed of fibers with either concrete or steel materials. Actual material properties at the time of the test were used in the model (Table 4.2). Confinement provided by the stirrups in the columns and beams was accounted for, using Mander’s confinement theory (Mander et al. 1988). The response of the concrete was modeled with the Kent-Scott-Park

concrete material (Scott et al. 1982), and concrete failure was considered to occur when the crushing strength in compression was reached. The response of the reinforcing steel was modeled using a Giuffre-Menegotto-Pinto steel material with isotropic strain hardening (Menegotto and Pinto, 1973), and the failure criterion for steel reinforcement was fracture in tension.

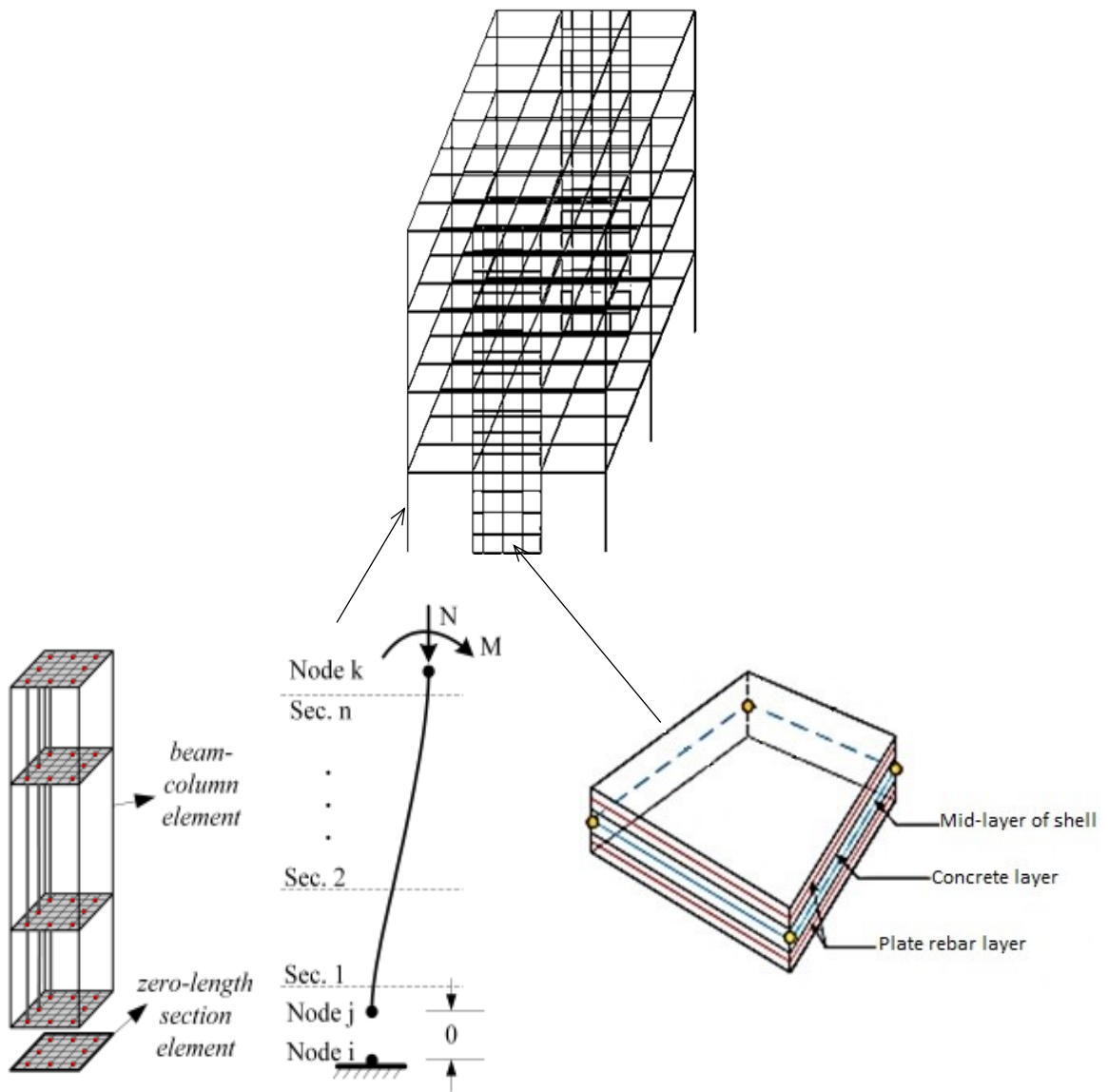


Figure 4.9. FEA model of RC building

The shear walls at each story were built using 16 four-node rectangular shell elements each, such that the size of the elements is 700 x 700 mm. The response of the concrete was modeled with the new Mazars concrete damage material, and the reinforcing steel was defined as a uniformly-distributed reinforcement ratio within the shell elements.

The nodes at the base were fixed in every degree of freedom, although bond-slip behaviour as proposed by Wehbe et al. (1997), was considered at the base of the columns, using zero-length elements with a hysteretic material with each of the sections properties. The load pattern in the finite element model is defined in two steps. First, the gravitational load was applied at the horizontal members and set constant. Then, the ground motions in each direction were created and imposed to all the base nodes.

The transient analysis was performed using a Newton algorithm, with a Newmark integrator to solve the systems of equations. This solution scheme has shown to perform better in complex structures, having fewer convergence problems in transient analyses. The damping of the structure was defined using Rayleigh Reitz damping of 2.0% in the first three modes of vibration. The nodal displacement and corresponding forces were recorded at each converged step, and the stress and strain of the elements were monitored.

4.4.2 Comparison of Predictions and Experimental Results

The results presented are obtained in both the longitudinal and transverse direction of the building, with the lateral support provided by the moment-frame system, and shear walls respectively (Fig. 4.10).

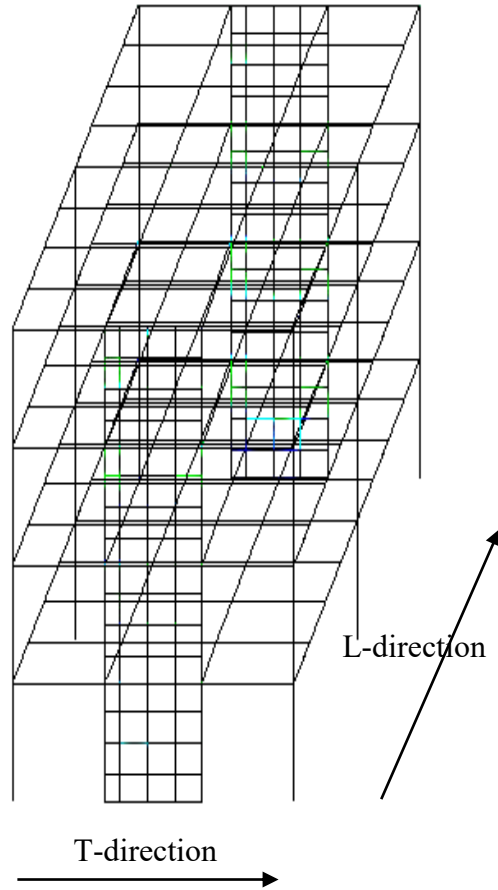


Figure 4.10. Transverse (T) and Longitudinal (L) directions of RC building

Figures 4.11, 4.12 and 4.13 show the comparisons of the analytical results with the experimental results for the reinforced concrete model, in terms of base shear for the 25%, 50%, and 100% Kobe records. Figure 4.11 indicates that the model is capable of capturing the global base shear response of the RC building for the 25% Kobe record in both the longitudinal and the transverse directions, which is essentially elastic. Similarly, the base shear for the 50% Kobe record was captured accurately, as seen in Fig. 4.12, whereas for the 100% Kobe (Fig. 4.13) record, the forces are generally overestimated at the peak acceleration of the motion. One possible explanation of the overestimation of the base shear forces is that neglecting the deformations associated with sliding at the wall base

creates a stiffer structure that dissipates less energy at the peak accelerations of the motion. Another potential factor affecting the results is the inability of the Mazars model to register any residual strain, again diminishing the energy dissipation capacity of the structure, particularly on the transverse direction.

For all three records, the overall force in both directions is reasonably captured by the model, although strength degradation at peak accelerations is moderately overestimated for the 100% Kobe record.

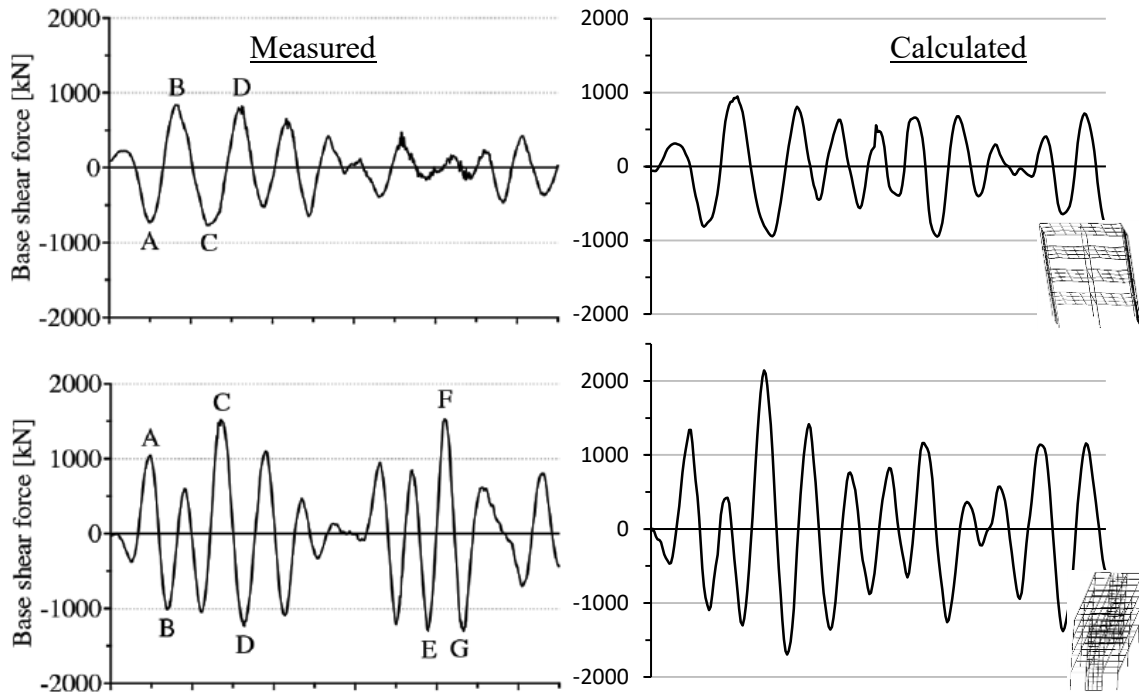


Figure 4.11. RC building base shear measured and calculated with 25% Kobe in a) longitudinal, and b) transverse directions

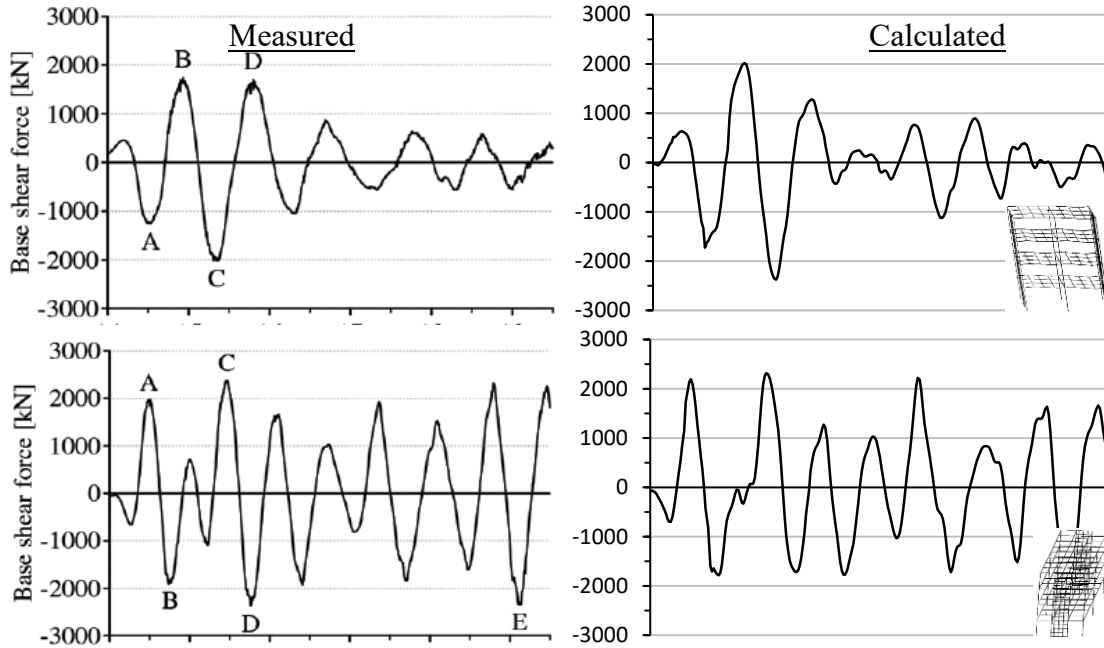


Figure 4.12. RC building base shear measured and calculated with 50% Kobe in a) longitudinal, and b) transverse directions

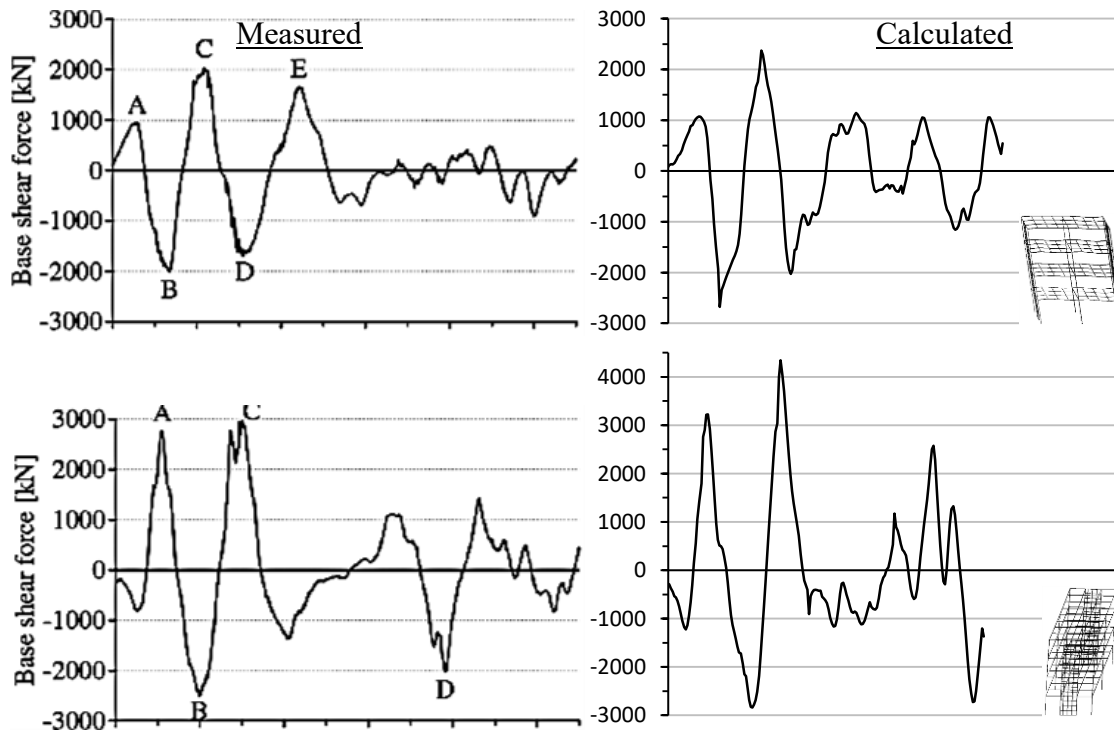


Figure 4.13. RC building base shear measured and calculated with 100% Kobe in a) longitudinal, and b) transverse directions

Table 4.3 shows the measured and calculated distribution of the maximum global roof drifts of the reinforced concrete building. They were estimated at the centre of the roof floor in both the longitudinal and the transverse directions. The maximum calculated roof drift for the 25% Kobe record is overestimated in both directions, while the drifts for the 50% and 100% records underestimate those of the test.

Input wave	Maximum roof drift measured		Maximum roof drift calculated	
	L-direction, mm	T-direction, mm	L-direction, mm	T-direction, mm
JMA-Kobe 25%	16.9	24.2	21.78	39.84
JMA-Kobe 50%	122.4	106.9	84.52	84.67
JMA-Kobe 100%	242.7	323.9	182.54	313.82

Table 4.3. Maximum roof drifts for RC building

Some potential reasons for this discrepancy in the results include the model's inability to predict shear deformations of the uniaxial elements present in columns and beams in the longitudinal direction, as well as the fact that sliding at the base of the shear walls in the transverse direction is not considered. This gives the structure a stiffer behaviour and decreases the displacements on each story. However, the results obtained have reasonable accuracy for all three intensities of the motion and resemble the actual behaviour of the RC structure.

4.5 Summary

The comparison of the models in OpenSees using the Mazars model for the biaxial behaviour of concrete with the results from literature tests, show that the Mazars model can capture the general response of different types of RC structures subjected to various loading

conditions. The maximum strength and displacement of the structures is predicted with reasonable accuracy; however, the model does not capture the energy dissipation capabilities of concrete accurately, nor it attempts to describe the cracking mechanism of these structures.

Chapter 5 – SUMMARY, CONCLUSIONS AND FUTURE WORK

This chapter summarizes the content of the thesis and gives the conclusions drawn from the research. Furthermore, a discussion of future research that will support advancement of this work is presented.

5.1 Summary

The thesis presents the implementation of the Mazars model, for the behaviour of concrete in two dimensions in finite element analysis, in the open-source, FEA framework OpenSees. The Mazars model is a damage-based material model that is simple enough for modelling RC structures at the system level, yet reasonably accurate. OpenSees allows users to expand and modify its source code in a modular fashion. The new material model is able to describe the behaviour of concrete in two dimensions in a simple way with a reasonable accuracy, which can be used with a multilayer-shell element in the modelling of complex 3D RC structures subjected to extreme loading.

An assessment of some of the most prominent element formulations for the biaxial behaviour of concrete in FEA is presented in Chapter 2. The uniaxial and biaxial behaviour of concrete is briefly explained, giving the background of the efforts in research to create a material model for the use in the FEA analysis of RC structures. The advantages and disadvantages of these theories and the finite element programs for the nonlinear analysis of structures, are discussed. Then, the presentation of the selected material model for this research is made in Chapter 3. The description of the element formulations by the Mazars

concrete damage model were given, and parametric analyses for the influence of its variables were shown. The element formulations were adapted for the use in a plane-stress element, and it was implemented in the OpenSees framework for the use in multilayer-shell elements (ShellMITC4). Last, the evaluation of the new Mazars model in OpenSees is presented in Chapter 4. Comparison of the results of analyses of RC structures using this model with experimental results from the literature indicates that the Mazars model can capture the general response parameters of RC structures subjected to monotonic, cyclic and dynamic loads, in terms of peak displacement and strength, in a fast manner without convergence problems.

5.2 Conclusions

The following conclusions can be drawn from the work presented in this thesis:

1. Current concrete models implemented in FEA are not suitable for the analysis at the system level of complex RC structures subjected to extreme loading without numerical-convergence problems.
2. The new Mazars concrete damage model is a rational and appropriate model capable of predicting the behaviour of concrete plane stress elements, using simple calculations that do not require complex solution algorithms within the element formulations.
3. Concrete compressive and tensile stress-strain response can be accurately described with the model by adjusting the material parameters (E_c , ε_{D0} , A_c , B_c , A_t , B_t).

4. Open-source, finite element analysis programs are useful tools for the implementation of material models that are simple, yet accurate in the representation of the behaviour of RC structures at the system level.
5. The response of the FEA model of a RC beam showed satisfactory agreement with the test results. The failure load and deflection of the beam were predicted successfully. However, the dependency of the tensile and compressive behaviour in the same variable (ϵ_{D0}) makes the model overestimate the cracking and yielding moment.
6. The maximum strength and displacement at each cycle of a RC shear wall under reverse-cyclic loading were calculated with the FEA model, showing moderate agreement with the measured response. The model failed to predict the energy dissipation capacity and residual displacement of the specimen.
7. The overall response of the RC building subjected to earthquake loading was predicted with reasonable accuracy. The shear force and roof displacements resemble the measured ones throughout the loading history.
8. The damage in the model affects the stiffness of the material exclusively, not considering residual (plastic) strains, nor it attempts to describe the cracking mechanism. Therefore, cyclic behaviour of the material fails to represent energy dissipation that would be characteristic of a concrete material.
9. The overall behaviour of concrete is well represented with the new Mazars model in OpenSees for analysis at the system level of RC structures, without numerical-convergence problems. Detailed information at every stage, such as crack mechanisms or energy dissipation, is not very well represented.

5.3 Future Work

Several ideas for future studies could be suggested based on the work presented in this research.

1. Currently, the material model is not capable of representing residual (plastic) strains. A damage model that separates the “elastic” and “plastic” parts of the compressive concrete curve can address this issue.
2. An explicit relationship to represent better the behaviour of the material when is subjected to shear, instead of exclusively using the β factor.
3. The complete separation of the tensile behaviour from the compressive behaviour by defining two damage-strain thresholds (ε_{D0}).
4. A study of the correlation of the parameters necessary to model the concrete curves using the Mazars model (E_c , ε_{D0} , A_c , B_c , A_t , B_t), with the parameters commonly obtained from concrete tests (f'_c , ε_0 , f_t).

REFERENCES

Abaqus FEA. (2009, May). *Abaqus Analysis User's Manual*.

<http://abaqusdoc.ualgary.ca/v6.9/books/usb/default.htm?startat=pt05ch19s06abm38.html>. Retrieved from

<http://abaqusdoc.ualgary.ca/v6.9/books/usb/default.htm?startat=pt05ch19s06abm38.html>

Ahmed, A. (2014). Modelling of a reinforced concrete beam subjected to impact vibration using ABAQUS. *International Journal of Civil and Structural Engineering*, 4(3).

AIJ. (1990). Design Guidelines for Earthquake Resistant Reinforced Concrete Buildings Based on the Inelastic Displacement Concept. Tokyo, Japan: Architectural Institute of Japan.

AIJ. (2010). Standard for Structural Calculation of Reinforced Concrete Structures. Tokyo, Japan: Architectural Institute of Japan.

Ali, A., Kim, D., & Cho, S. (2013, February). Modeling of nonlinear cyclic load behavior of I-shaped composite steel-concrete shear walls of nuclear power plants. *Nuclear Engineering and Technology*, 45(1), 89-98.

Attard, M., & Mendis, P. (1993). Ductility of High Strength Concrete Columns. *Australian Civil Engineering Transactions*, 295-306.

- Ayoub, A., & Filippou, F. (1998, March). Nonlinear Finite-Element Analysis of RC Shear Panels and Walls. *Journal of Structural Engineering, ASCE*, 124(3), 298-308.
- Dvorkin, E., Pantuso, D., & Repetto, E. (1995). A formulation of the MITC4 shell element for finite strain elasto-plastic analysis. *Comput. Methods Appl. Mec. Eng.*, 125(1), 17-40.
- Ebead, U., & Neale, K. (2005). Interfacial behaviour of FRP-concrete joints subjected to direct shear. *Proceedings, Annual Conference - Canadian Society for Civil Engineering*.
- Fenves, G. (2001). *Annual Workshop on Open System for Earthquake Engineering Simulation*. (P. E. Center, Ed.) Retrieved from <http://opensees.berkeley.edu/>
- Genikomsou, A., & Polak, M. (2014). Finite Element Analysis of a Reinforced Concrete Slab-Column Connection using ABAQUS. *Structures Congress, ASCE*.
- Hamon, F. (2013). *Code Aster: Mazars Damage Model Revision 10461*. Retrieved from http://www.code-aster.org/doc/v11/en/man_r/r7/r7.01.08.pdf
- Han, J., Li, Z., & Song, J. (2010). The application of finite element analysis software (ABAQUS) in structural analysis. *International Conference on Computational and Information Sciences*. Chengdu, China.
- Hiotakis, S. (2004). Repair and Strengthening of Reinforced Concrete Shear Walls for Earthquake Resistance Using Externally Bonded Carbon Fibre Sheets and a Novel

Anchor System. *Master's thesis, Department of Civil and Environmental Engineering.*

Hognestad, E. (1951). A study on combined bending and axial load in reinforced concrete members. *University of Illinois Engineering Experiment Station*, 43-46.

Hsu, T., & Mo, Y. (2010). *Unified Theory of Concrete Structures*. Houston: John Wiley and Sons Ltd.

Hsu, T., & Zhu, R. (2002). Softened Membrane Model for Reinforced Concrete Elements in Shear. *Structural Journal of the American Concrete Institute*, 99(4), 460-469.

Izumo, J., Shin, H., Maekawa, K., & Okamura, H. (1992). An Analytical Model for RC Panels Subjected to In-plane Stresses. *Proceedings of the International Workshop on Concrete Shear in Earthquake* (pp. 206-215). Houston: Elsevier Science Publishers, Inc.

Kachanov, L. (1958). Time of the rupture process under creep conditions. *Izv. Akad. Nauk SSR Otd.*, 8, 26-31.

Karsan, P., & Jirsa, J. (1969, December). Behavior of Concrete under Compressive Loading. *Journal of Structural Division, ASCE*, 95(ST12), 2543-2563.

Kent, D., & Park, R. (1971). Flexural members with confined concrete. *Journal of the Structural Division, ASCE*, 97(ST7), 1969-1990.

Lee, H., & Kuchma, D. (2007). Seismic overstrength of shear walls in parking structures with flexible diaphragms. *Journal of Earthquake Engineering*, 11(1), 86-109.

doi:10.1080/13632460601033488

- Legeron, F., Paultre, P., & Mazars, J. (2005). Damage Mechanics Modeling of Nonlinear Seismic Behavior of Concrete Structures. *Journal of Structural Engineering, ASCE*, 131(6), 946-955.
- Lemaitre, J. (1992). *A Course on Damage Mechanics*. Springer-Verlag.
- Li, Z. (2011). *Advanced Concrete Technology*. John Wiley and Sons Ltd.
- Loland, K. (1980). Continuous damage model for load-response estimation of concrete. *Cement. Concr. Res.*, 10(3), 395-402.
- Lu, X., Xie, L., Guan, H., & Lu, X. (2015, June). A Shear Wall Element for Nonlinear Seismic Analysis of Super-Tall Buildings Using OpenSees. *Finite Element in Analysis and Design*, 98, 14-25.
- Luu, H., Ghorbanirenani, I., Leger, P., & Tremblay, R. (2013). Numerical Modeling of Slender Reinforced Concrete Shear Wall Shaking Table Tests Under High-Frequency Ground Motions. *Journal of Earthquake Engineering*, 17(4), 517-542. doi:10.1080/13632469.2012.767759
- Mander, J., Priestly, M., & Park, R. (1988). Theoretical Stress-strain Model of Confined Concrete. *Journal of Structural Engineering*, 114(8), 1804-1826.
- Mansour, M., & Hsu, T. (2005). Behavior of Reinforced Concrete Elements under Cyclic Shear: Part 2 - Theoretical Model. *Journal of Structural Engineering, ASCE*, 131(1), 54-65.

- Mazars, J. (1984). Application de la mecanique de l'endommagement au compportement non lineaire et a la ruptura du beton de structure. *These de Doctorate d'Etat, L.M.T., Universite Paris, France.*
- Mazars, J., Hamon, F., & Grange, S. (2015). A new 3D damage model for concrete under monotonic, cyclic and dynamic loading. *Materials and Structures, 48*, 3779-3793.
- Mazars, J., Kotronis, P., & Davenne, L. (2002). A new modelling strategy for the behaviour of shear walls dynamic loading. *Earthquake Engineering and Structural Dynamics, 31*, 937-954.
- Menegotto, M., & Pinto, P. (1973). Method of Analysis for Cyclically Loaded Reinforced Concrete Plane Frames Including Changes in Geometry and Nonelastic Behavior of Elements under Combined Normal Forced and Bending. *IABSE Symposium on Resistance and Ultimate Deformability of Structres Acted on by Well-Defined Repetead Loads*. Lisbon, Portugal.
- Mergos, P., & Beyer, K. (2013). Modelling shear-flexure interaction in equivalent frame models of slender reinforced concrete walls. In *Struct. Design Tall Spec. Build.* Wiley Library. doi:10.1002/TAL.1114
- Nagae, T., Ghannoum, W., Kwon, J., Tahara, K., Fukuyama, K., Matsumori, T., . . . Moehle, J. (2015, March-April). Design Implications of Large-Scale Shake-Table Test on Four-Story Reinforced Concrete Building. *ACI Structural Journal* , *112*(S12), 135-146.
- Nagae, T., Tahara, K., Fukuyama, K., Matsumori, T., Shiohara, H., Kabeyasawa, T., . . . Nishiyama, I. (2011a). Large-Scale Shaking Table Tests on A Four-Story RC

- Building. *Journal of Structural and Construction Engineering*, 76(669), 1961-1970.
- Nagae, T., Tahara, K., Taiso, M., Shiohara, H., Kabeyasawa, T., Kono, S., . . . Tuna, Z. (2011b). Design and Instrumentation of the 2010 E-Defense Four-Story Reinforced Concrete and Post-Tensioned Concrete Buildings. *PEER Report*, 104, 261.
- Palermo, D., & Vecchio, F. (2003, Sept.-Oct.). Compression Field Modeling of Reinforced Concrete Subjected to Reversed Loading: Formulation. *ACI Structural Journal*, 100(5), 616-625.
- Pang, B., & Hsu, T. (1996). Fixed Angle Softened Truss Model for Reinforced Concrete. *ACI Structural Journal*, 93(2), 197-207.
- Scott, B., Park, R., & Priestly, M. (1982). Stress-strain Behavior of Concrete Confined by Overlapping Hoops at Low and High Strain Rates. *ACI Journal*, 79(1), 13-27.
- Scott, M., & Fenves, G. (2003). A Krylov Subspace Accelerated Newton Algorithm. *ASCE Structures Congress*. Seattle, WA.
- Tasuji, M., Slate, F., & Nilson, A. (1978, December). Stress-Strain Response and Fracture of Concrete in Biaxial Loading. *Proc. Am. Concr. Inst.*, 69(12), 758-764.
- Tuna, Z., Gavridou, S., Wallace, J., Nagae, T., & Matsumori, T. (2012). 2010 E-Defense Four-Story Reinforced Concrete and Post-Tensioned Buildings - Preliminary Comparative Study of Experimental and Analytical Results. *15 WCEE*. Lisbon, Portugal.

- Vecchio, F. (2000). Disturbed stress field model for reinforced concrete: Formulation. *J. Struct. Engrg., ASCE*, 126(9), 1070-1077.
- Vecchio, F., & Collins, M. (1982). *Response of Reinforced Concrete to In-Plane Shear and Normal Stresses*. Toronto, Canada: University of Toronto.
- Vecchio, F., & Collins, M. (1986, Mar.-Apr.). The Modified Compression-Field Theory for Reinforced Concrete Elements Subjected to Shear. *ACI Journal, Proceedings*(83), 219-231.
- Vecchio, F., Lai, D., Sim, W., & Ng, J. (2001, April). Disturbed Stress Field Model for Reinforced Concrete: Validation. *Journal of Structural Engineering, ASCE*, 127(4), 350-358.
- Wehbe, N., Saiidi, M., & Sanders, D. (1997, September). Effect of Confinement and Faires on the Seismic Performance of Reinforced Concrete Bridge Columns. *Civil Engineering Department, Report No. CCEER-97-2*.
- Wischers, G. (1978). Application of Effects of Compressive Loads on Concrete. *Bentotech. Ber.*(2 and 3).
- Wong, P., Vecchio, F., & Trommels, H. (2013). *VecTor2 & FormWorks user's manual. Second Edition*.
- Zhang, H., & Li, H. (2012). Shaking table test and dynamic response analysis of reinforced concrete structure. *15 WCEE*. Lisbon.
- Zhong, J. (2005). Model-Based Simulation of Reinforced Concrete Plane Stress Structures. *PhD Thesis Dissertation. University of Houston*.

APPENDIX A – ‘MAZARS’ SOURCE CODE

A.1 Header File (Mazars.h)

```
#include <stdio.h>
#include <stdlib.h>
#include <math.h>
#include <Vector.h>
#include <Matrix.h>
#include <ID.h>
#include <NDMaterial.h>

class Mazars: public NDMaterial{
public :
    Mazars( ) ;
    Mazars(int tag, double _Ec, double _epsD0, double _Ac, double _Bc, double _At,
           double _Bt, double _nu) ;

    virtual ~Mazars( ) ;

    void setInitials( ) ;

    //make a clone of this material
    NDMaterial *getCopy( ) ;
    NDMaterial *getCopy( const char *type ) ;

    //send back order of strain in vector form
    int getOrder( ) const ;

    //send back order of strain in vector form
    const char *getType( ) const ;

    //swap history variables
    int commitState( ) ;

    //revert to last saved state
    int revertToLastCommit( ) ;

    //revert to start
    int revertToStart( ) ;

    //get the strain
    int setTrialStrain( const Vector &strainFromElement ) ;

    //send back the strain
    const Vector& getStrain( ) ;

    //send back the stress
    const Vector& getStress( ) ;

    //send back the tangent
    const Matrix& getTangent( ) ;

    const Matrix& getInitialTangent( ) ;
```

```
//print out data
void Print( OPS_Stream &s, int flag ) ;

int sendSelf(int commitTag, Channel &theChannel);
int recvSelf(int commitTag, Channel &theChannel, FEM_ObjectBroker &theBroker);

private :
Matrix iniTangent, tTangent, cTangent, iniSmallTangent, tangent;
Matrix iniTangentInv, tTangentInv, cTangentInv;
Vector tStrain, cStrain, strain, tStress, cStress, stress;
double nu, Ec, epsD0, Ac, Bc, At, Bt, Beta;
double fac, tDam, cDam, tepseq, cepseq;

} ;
```

A.2 C++ File (Mazars.cpp)

```
#include <elementAPI.h>
#include <Mazars.h>
#include <Channel.h>
#include <FEM_ObjectBroker.h>
#include <MaterialResponse.h>

#include <OPS_Globals.h>
#include <Information.h>
#include <Parameter.h>
#include <string.h>
#include <Vector.h>
#include <math.h>
#include <float.h>
#include <Matrix.h>

#include <iostream>

void *
OPS_Mazars(void)
{
    NDMaterial *theMaterial = 0;

    int numArgs = OPS_GetNumRemainingInputArgs();

    if (numArgs != 8) {
        opserr << "Want: nDMaterial Mazars tag? Ec? epsD0? Ac? Bc? At? Bt? nu?" << endl;
        return 0;
    }

    int iData[1];
    double dData[7];

    int numData = 1;
    if (OPS_GetInt(&numData, iData) != 0) {
        opserr << "WARNING invalid integer tag: nDMaterial Mazars \n";
        return 0;
    }

    numData = 7;

    if (OPS_GetDouble(&numData, dData) != 0) {
        opserr << "WARNING invalid data: nDMaterial Mazars : " << iData[0] << "\n";
        return 0;
    }

    theMaterial = new Mazars(iData[0], dData[0], dData[1], dData[2], dData[3], dData[4],
                            dData[5], dData[6]);

    return theMaterial;
}

//null constructor
Mazars::Mazars( ) :
    NDMaterial(0, ND_TAG_Mazars ),
    tStrain(6), cStrain(6), tStress(6), cStress(6), strain(3), stress(3),
    tTangent(6,6), cTangent(6,6), tangent(3,3), tTangentInv(6,6), cTangentInv(6,6),
    iniTangent(6,6), iniSmallTangent(3,3), iniTangentInv(6,6)
{ }
```

```

//full constructor
Mazars::Mazars(int tag, double _Ec, double _epsD0, double _Ac, double _Bc, double _At,
               double _Bt, double _nu) :

NDMaterial( tag, ND_TAG_Mazars ),
tStrain(6), cStrain(6), tStress(6), cStress(6), strain(3), stress(3),
tTangent(6,6), cTangent(6,6), tangent(3,3), tTangentInv(6,6), cTangentInv(6,6),
iniTangent(6,6), iniSmallTangent(3,3), iniTangentInv(6,6),
Ec(_Ec), epsD0(_epsD0), Ac(_Ac), Bc(_Bc), At(_At), Bt(_Bt), nu(_nu)
{
    setInitials();
}

//destructor
Mazars::~Mazars( )
{

}

void Mazars::setInitials()
{

    if (Ec < 0.0)
        Ec = -Ec;
    if (epsD0 < 0.0)
        epsD0 = -epsD0;
    Beta = 1.06;

    tStrain.Zero();
    cStrain = tStrain;
    strain.Zero();

    tStress.Zero();
    cStress = tStress;
    stress.Zero();

    iniTangent.Zero();
    iniTangent(0,0) = 1.0 - nu;
    iniTangent(0,1) = nu;
    iniTangent(0,2) = nu;
    iniTangent(1,0) = nu;
    iniTangent(1,1) = 1.0 - nu;
    iniTangent(1,2) = nu;
    iniTangent(2,0) = nu;
    iniTangent(2,1) = nu;
    iniTangent(2,2) = 1.0 - nu;
    iniTangent(3,3) = (1.0 - 2.0 * nu) / 2.0;
    iniTangent(4,4) = (1.0 - 2.0 * nu) / 2.0;
    iniTangent(5,5) = (1.0 - 2.0 * nu) / 2.0;
    fac = Ec / ((1.0 + nu) * (1.0 - 2.0 * nu));
    iniTangent *= fac;

    iniTangentInv.Zero();
    iniTangentInv(0,0) = 1.0 / Ec;
    iniTangentInv(0,1) = - nu / Ec;
    iniTangentInv(0,2) = - nu / Ec;
    iniTangentInv(1,0) = - nu / Ec;
    iniTangentInv(1,1) = 1.0 / Ec;
    iniTangentInv(1,2) = - nu / Ec;
    iniTangentInv(2,0) = - nu / Ec;
}

```

```

iniTangentInv(2,1) = - nu / Ec;
iniTangentInv(2,2) = 1.0 / Ec;
iniTangentInv(3,3) = (2 * (1 + nu)) / Ec;
iniTangentInv(4,4) = (2 * (1 + nu)) / Ec;
iniTangentInv(5,5) = (2 * (1 + nu)) / Ec;

iniSmallTangent.Zero();
iniSmallTangent(0,0) = iniTangent(0,0);
iniSmallTangent(0,1) = iniTangent(0,1);
iniSmallTangent(1,0) = iniTangent(1,0);
iniSmallTangent(1,1) = iniTangent(1,1);
iniSmallTangent(2,2) = iniTangent(3,3);

tDam = 0;
cDam = 0;
tepeq = 0;
cepeq = 0;
tTangent = iniTangent;
cTangent = tTangent;
tTangentInv = iniTangentInv;
cTangentInv = tTangentInv;
tangent = iniSmallTangent;
}

//make a clone of this material
NDMaterial*
Mazars::getCopy( )
{
    Mazars *clone ;    //new instance of this class

    clone = new Mazars( this->getTag(), Ec, epsD0, Ac, Bc, At, Bt, nu);

    return clone ;
}

//make a clone of this material
NDMaterial*
Mazars::getCopy( const char *type )
{
    return this->getCopy( ) ;
}

//send back order of strain in vector form
int
Mazars::getOrder( ) const
{
    return 3 ;
}

const char*
Mazars::getType( ) const
{
    return "Mazars" ;
}

//swap history variables
int
Mazars::commitState( )
{

```

```

cStress = tStress;
cStrain = tStrain;
cTangent = tTangent;
cTangentInv = tTangentInv;
cDam = tDam;
cepseq = tepseq;

return 0;
}

//revert to last saved state
int
Mazars::revertToLastCommit( )
{
return 0;
}

//revert to start
int
Mazars::revertToStart( )
{
cStrain.Zero();
tStrain.Zero();
strain.Zero();
cStress.Zero();
tStress.Zero();
stress.Zero();

setInitials();

return 0;
}

//receive the strain
int
Mazars::setTrialStrain( const Vector &strainFromElement )
{
double psi, epsL1, epsL2, epsL3, epseq2 ;
double H1, H2, H3, alphas, alphac, DamT, DamC ;
static Vector epsp(6), sigep(6), sigpos(6), signeg(6), epst(6), epsc(6), sigp(6) ;

tStrain(0) = strainFromElement(0) ;
tStrain(1) = strainFromElement(1) ;
tStrain(3) = strainFromElement(2) ;

tStrain(2) = (- nu / Ec) * (tStress(0) + tStress(1)) ;

tTangent = cTangent ;
tTangentInv = cTangentInv;

psi = (atan (2 * tStrain(3) / (tStrain(0) - tStrain(1) + 1e-20))) / 2;

epsp.Zero();
epsp(0) = ((tStrain(0) + tStrain(1)) / 2) + (((tStrain(0) - tStrain(1)) / 2) * cos (2
* psi)) + (tStrain(3) * sin (2 * psi)) ;
epsp(1) = ((tStrain(0) + tStrain(1)) / 2) - (((tStrain(0) - tStrain(1)) / 2) * cos (2
* psi)) - (tStrain(3) * sin (2 * psi)) ;
epsp(2) = tStrain(2) ;

if (epsp(0) >= 0)
    epsL1 = epsp(0);

```

```

else
    epsL1 = 0;

if (epsp(1) >= 0)
    epsL2 = epsp(1);
else
    epsL2 = 0;

if (epsp(2) >= 0)
    epsL3 = epsp(2);
else
    epsL3 = 0;

epseq2 = pow(epsL1, 2) + pow(epsL2, 2) + pow(epsL3, 2) ;
tepseq = sqrt(epseq2) ;
epseq2 += 1e-20 ; // Avoids dividing by zero

if ( tepseq > cepseq )
{
    sigep = tTangent * epsp ;

    sigpos.Zero();
    signeg.Zero();

    if (sigep(0) >= 0)
    {
        sigpos(0) = sigep(0);
        signeg(0) = 0;
    }
    else
    {
        sigpos(0) = 0;
        signeg(0) = sigep(0);
    }

    if (sigep(1) >= 0)
    {
        sigpos(1) = sigep(1);
        signeg(1) = 0;
    }
    else
    {
        sigpos(1) = 0;
        signeg(1) = sigep(1);
    }

    if (sigep(2) >= 0)
    {
        sigpos(2) = sigep(2);
        signeg(2) = 0;
    }
    else
    {
        sigpos(2) = 0;
        signeg(2) = sigep(2);
    }

    epst = tTangentInv * sigpos ;
    epsc = tTangentInv * signeg ;
}

```

```

if (epst(0) + epsc(0) >= 0)
    H1 = 1;
else
    H1 = 0;

if (epst(1) + epsc(1) >= 0)
    H2 = 1;
else
    H2 = 0;

if (epst(2) + epsc(2) >= 0)
    H3 = 1;
else
    H3 = 0;

alphanat = (H1 * epst(0) * (epst(0) + epsc(0)) / epseq2) + (H2 * epst(1) *
    (epst(1) + epsc(1)) / epseq2) + (H3 * epst(2) * (epst(2) + epsc(2)) /
    epseq2) ;
alphac = (H1 * epsc(0) * (epst(0) + epsc(0)) / epseq2) + (H2 * epsc(1) *
    (epst(1) + epsc(1)) / epseq2) + (H3 * epsc(2) * (epst(2) + epsc(2)) /
    epseq2) ;

if ( tepseq > epsD0 )
{
    DamC = 1.0 - (epsD0 * (1.0 - Ac) / tepseq) - Ac * exp(-Bc * (tepseq -
        epsD0)) ;
    DamT = 1.0 - (epsD0 * (1.0 - At) / tepseq) - At * exp(-Bt * (tepseq -
        epsD0)) ;

    tDam = pow(alphanat, Beta) * DamT + pow(alphac, Beta) * DamC ;
}
}

if ( tDam < 0.0 )
    tDam = 0.0;
if ( tDam > 0.9999 )
    tDam = 0.9999;
if ( tDam < cDam )
    tDam = cDam;

tTangent = (1.0 - tDam) * iniTangent ;
tTangentInv = (1.0 / (1.0 - tDam)) * iniTangentInv ;
sigp = tTangent * epsp ;

tStress(0) = 0.5 * (sigp(0) + sigp(1)) + 0.5 * (sigp(0) - sigp(1)) * cos(2.0 * (-
    psi)) ;
tStress(1) = 0.5 * (sigp(0) + sigp(1)) - 0.5 * (sigp(0) - sigp(1)) * cos(2.0 * (-
    psi)) ;
tStress(3) = -0.5 * (sigp(0) - sigp(1)) * sin(2.0 * (-psi)) ;

tangent(0,0) = tTangent(0,0);
tangent(0,1) = tTangent(0,1);
tangent(1,0) = tTangent(1,0);
tangent(1,1) = tTangent(1,1);
tangent(2,2) = tTangent(3,3);

strain(0) = tStrain(0);
strain(1) = tStrain(1);
strain(2) = tStrain(3);

stress(0) = tStress(0);

```

```

    stress(1) = tStress(1);
    stress(2) = tStress(3);

    return 0;
}

//send back the strain
const Vector&
Mazars::getStrain( )
{
    return strain ;
}

//send back the stress
const Vector&
Mazars::getStress( )
{
    return stress ;
}

//send back the tangent
const Matrix&
Mazars::getTangent( )
{
    return tangent ;
}

const Matrix&
Mazars::getInitialTangent
( )
{
    return iniSmallTangent ;
}

//print out data
void
Mazars::Print( OPS_Stream &s, int flag )
{
    s << "Mazars Material tag: " << this->getTag() << endln ;
    s << " Ec: " << Ec << " ";
    s << " epsD0: " << epsD0 << " ";
    s << " Ac: " << Ac << " ";
    s << " Bc: " << Bc << " ";
    s << " At: " << At << " ";
    s << " Bt: " << Bt << " ";
    s << " nu: " << nu << " ";
}

int
Mazars::sendSelf(int commitTag, Channel &theChannel)
{
    int res = 0, cnt = 0;

    static Vector data(21);

    data(cnt++) = this->getTag();
    data(cnt++) = Ec;
    data(cnt++) = epsD0;
    data(cnt++) = Ac;
    data(cnt++) = Bc;
    data(cnt++) = At;

```

```

data(cnt++) = Bt;
data(cnt++) = nu;
data(cnt++) = cDam;

int i;
for (i = 0; i < 6; i++)
    data(cnt++) = cStrain(i);

for (i = 0; i < 6; i++)
    data(cnt++) = cStress(i);

res = theChannel.sendVector(this->getDbTag(), commitTag, data);
if (res < 0)
    opserr << "Mazars::sendSelf() - failed to send data" << endl;

return res;
}

int
Mazars::recvSelf(int commitTag, Channel &theChannel, FEM_ObjectBroker &theBroker)
{
    int res = 0, cnt = 0;

    static Vector data(21);

    res = theChannel.recvVector(this->getDbTag(), commitTag, data);
    if (res < 0) {
        opserr << "Mazars::recvSelf -- could not recv Vector" << endl;
        return res;
    }

    this->setTag(int(data(cnt++)));
    Ec = data(cnt++);
    epsD0 = data(cnt++);
    Ac = data(cnt++);
    Bc = data(cnt++);
    At = data(cnt++);
    Bt = data(cnt++);
    nu = data(cnt++);
    cDam = data(cnt++);

    setInitials();

    int i;
    for (i = 0; i < 6; i++)
        cStrain(i) = data(cnt++);

    for (i = 0; i < 6; i++)
        cStress(i) = data(cnt++);

    return res;
}

```